Top Curr Chem (2013) 328: 99–154
DOI: 10.1007/128_2012_323

Published online: 11 May 2012

Allostery in the Hsp70 Chaperone Proteins

Erik R. P. Zuiderweg, Eric B. Bertelsen, Aikaterini Rousaki, Matthias P. Mayer, Jason E. Gestwicki, and Atta Ahmad

Abstract Heat shock 70-kDa (Hsp70) chaperones are essential to in vivo protein folding, protein transport, and protein re-folding. They carry out these activities using repeated cycles of binding and release of client proteins. This process is under allosteric control of nucleotide binding and hydrolysis. X-ray crystallography, NMR spectroscopy, and other biophysical techniques have contributed much to the understanding of the allosteric mechanism linking these activities and the effect of co-chaperones on this mechanism. In this chapter these findings are critically reviewed. Studies on the allosteric mechanisms of Hsp70 have gained enhanced urgency, as recent studies have implicated this chaperone as a potential drug target

E.R.P. Zuiderweg (✉) and E.B. Bertelsen
Department of Biological Chemistry, The University of Michigan, Ann Arbor, MI 48109, USA
e-mail: zuiderwe@umich.edu

A. Rousaki
Program in Biophysics, The University of Michigan, Ann Arbor, MI 48109, USA

Institute of Organic Chemistry and Chemical Biology, Goethe University, Max-von-Laue-Str. 7, 60438 Frankfurt, DE

M.P. Mayer
Zentrum für Molekulare Biologie der Ruprecht-Karls-Universität Heidelberg, Heidelberg, Germany

J.E. Gestwicki
Department of Biological Chemistry, The University of Michigan, Ann Arbor, MI 48109, USA

Lifesciences Institute, The University of Michigan, Ann Arbor, MI 48109, USA

Department of Pathology, The University of Michigan, Ann Arbor, MI 48109, USA

A. Ahmad
Department of Biological Chemistry, The University of Michigan, Ann Arbor, MI 48109, USA

Lifesciences Institute, The University of Michigan, Ann Arbor, MI 48109, USA

in diseases such as Alzheimer's and cancer. Recent approaches to combat these diseases through interference with the Hsp70 allosteric mechanism are discussed.

Keywords Dynamics · DnaJ · DnaK · Interactions · Structure

Contents

1 General Introduction

Heat shock 70-kDa proteins, Hsp70s, were first identified in bacteria as being over-expressed in response to cellular stress such as elevated temperatures, nutrient deprivation, heavy metals, oxidative stress, and viral infections [1]. Hsp70s rescue proteins that have been partially denatured, misfolded, and/or have become aggregated by these conditions. Hsp70s can unfold these clients in a complicated process fueled by ATP hydrolysis under allosteric control [2]. The unfolded clients are then free to refold properly. In addition to their roles in the stress response, Hsp70s are also expressed in normal, unstressed cells, where they act as chaperones, catalyzing the overall folding yield of newly expressed proteins by unfolding off-pathway intermediates [3, 4].

Hsp70s occur in all domains of life: archaea, eubacteria, and eukaryotes. In the eukaryotes, (specialized) Hsp70s are found in the cytosol, nucleus, mitochondria, chloroplasts, and endoplasmic reticulum. Hsp70s have been shown to be the most conserved proteins found in all organisms [5]. In archaea and eubacteria Hsp70 is referred to as DnaK. In yeasts they are called SSA, in mammals including humans they are referred to as HSPA. The latter are enumerated in Table 1. Most species encode for at least three Hsp70s.

In stressed human cells, the 13 Hsp70 isoforms account for 2% of all protein mass [6]. In addition to Hsp70's role in protein re-folding, Hsp70s direct irreversibly denatured proteins to degradation by the ubiquitin-proteasome system [7] or by the lysosomal proteolysis system [8]. Hsp70s are assisted by co-chaperones called J-proteins (Hsp40) [9] and nucleotide exchange factors (NEF) [10]. Apart from

Table 1 Homology for the hydrophobic NBD-SBD linker for the human HSPA (HSPA8 count) as compared to Hsp110 of *S. cervicea* (bottom)

Systematic name	Old name	390	391	392	393	394	395	396	397	398
HspA1A	Hsp70 1A/1B	D	L	L	L	L	D	V	A	P
HspA1L	Hsp70 1-like	D	L	L	L	L	D	V	A	P
Hspa2	Hsp70 2	D	L	L	L	L	D	V	T	P
HSPA5	Grp78, Bip	D	L	V	L	L	D	V	C	P
HSPA6	Hsp70 6	D	L	L	L	L	D	V	A	P
HSPA8	Hsc70	D	L	L	L	L	D	V	T	P
HSPA9	Mt-Hsp70, mortalin	D	V	L	L	L	D	V	T	P
HSP12A	Hsp70 12A	A	V	I	K	V	R	R	S	P
HSPA12b	Hsp70 12B	G	V	V	R	V	R	R	S	P
HSPA13	Hsp70 13	A	L	E	I	P	N	K	H	L
HSPA14	Hsp70 14	D	S	L	M	I	E	C	S	A
		395	396	397	398	399	400	401	402	403
HSP110	SSB-1	E	D	I	H	P	Y	S	V	S

their function in protein (re)folding, the Hsp70 proteins also mediate uncoating of clathrin-coated vesicles [11], trafficking of nuclear hormone receptors [12], and antigen presentation by MHCs [13]. Because of these varied roles, Hsp70 is considered a core mediator of protein homeostasis.

Hsp70s have been implicated in numerous diseases. For example, Hsp70s are upregulated in tumors [14], and they are required for the survival of these cells [15–17]. Enhanced expression of Hsp70 in tumor cells is likely caused by conditions which mimic stress [18, 19]. Hsp70s are thought to play at least three roles in cancer. First, they are thought to attempt to neutralize the conformational changes in mutant proteins [20, 21] which are common in tumorigenic cells. Second, Hsp70s are found to inhibit specifically cell death pathways [19, 22–26]. Third, mitochondrial Hsp70 can directly inactivate p53 tumor suppressor protein [27, 28]. Hsp70s are also involved in several CNS disorders. Diseases such as Alzheimer's, Pick's disease, progressive supranuclear palsy, corticobasal degeneration, and argyrophilic grain disease are characterized by the aberrant accumulation of hyperphosphorylated tau, called tau-tangles [29]. Hsp70s participate in the clearance of tau-tangles through a mechanism that is currently not well understood. Because of these emerging roles of Hsp70s in multiple diseases, there is renewed interest in understanding the mechanisms of this chaperone, with the goal of creating new medicines that best exploit the complex mechanisms of allostery in the Hsp70 system.

2 Hsp70 Overall Architecture and ATP Hydrolysis

Because Hsp70s are extremely well conserved proteins (53% identity, 68% homology between the Hsp70 of *E. coli* and Hsc70 of humans), the conclusions of studies using an Hsp70 from one organism are often considered to approximate the behavior of the others. Thus, we primarily discuss the properties and allosterics

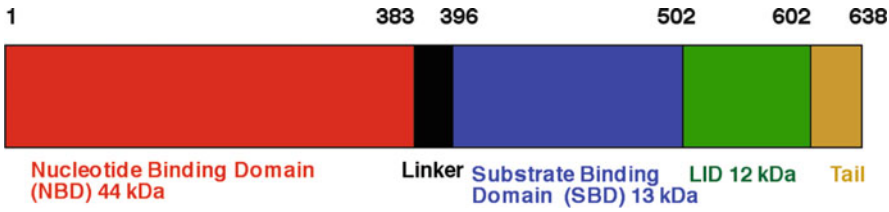

Fig. 1 Hsp70 domain architecture in DnaK *E. coli* count

of the Hsp70s in the context of the *E. coli* ortholog, called DnaK, because it is one of the best studied. Further, in this review we will often use the names DnaK and Hsp70 interchangeably.

DnaK contains three domains (see Fig. 1). The N-terminal 45-kDa Nucleotide Binding Domain (NBD) is formally divided into four subdomains: IA (1–37, 112–184, 363–383), IB (38–111), IIA (185–227, 310–362) and IIB (228–309), all in DnaK *E. coli* numbering. IA-IB and IIA-IIB form the two arms of a V-shaped structure [30, 31]. Nucleotide is bound at the center of the V-shaped cleft and is coordinated by residues derived from all four subdomains. The distribution is skewed: the adenosine and deoxy-ribose moieties are wedged into the interface of subdomains IIA and IIB. The α-phosphate and β-phosphate interact mostly with residues from subdomain IIA, whereas the γ-phosphate and the ATP-coordinated Mg^{2+} ion are mostly in contact with residues of subdomain IA. Only one residue from subdomain IB is involved in interaction with nucleotide. It is Lys70 which is absolutely essential for catalysis (Lys71 Hsc70 for which the definitive mutagenesis experiment was carried out [32]). The lysine ε-amino group is likely involved in the activation of the water molecule that carries out the nucleophilic attack on the gamma phosphate [32]. Mutations of other residues involved in nucleotide or Mg^{2+} binding affect k_{cat} and/or K_M, but no single mutation completely abolishes hydrolysis [33]. Hence there is no single residue acting as the sole general base catalyst. Even the nature of the monovalent ions that help coordinate the γ-phosphate in the active site is important: ATP hydrolysis is five times slower in NaCl than in KCl [34].

The NBD is connected via a linker to the Substrate Binding Domain (SBD). The linker is 10–12 residues in length and is highly conserved, showing a characteristic D/E-V/I/L-L-L-D-V-*-P hydrophobic sequence [35]. The SBD is a β-basket of 13 kDa, which is made up of two antiparallel β-sheets of four strands each [36]. The substrate-binding pocket is located between the two β sheets, is highly hydrophobic, and displays a high affinity for hydrophobic residues such as Leu [37]. A short linker connects the SBD to the 15-kDa alpha-helical LID which shields the substrate-binding pocket [37]. Beyond the LID is a tail region of varying length (approximately 50 residues) and sequence. In *E. coli* DnaK this tail is disordered and dynamic [38]. Recent work indicates that it may act as a disordered tether linked to a weak substrate-binding motif which enhances chaperone function by

transiently interacting with folding clients [39]. In human Hsp70s the very C-terminus of the tail region contains sequences that are important for the interaction with the CHIP [12], a ubiquitin ligase, or for ER targeting [40].

3 The Hsp70 Functional Cycle

Misfolded proteins (substrates) display stretches of exposed hydrophobic amino acids. The most quoted [41], but not universal [42], view is that co-chaperones of the DnaJ class (Hsp40) are the first to recognize and bind to such substrates, and escort them to the Hsp70 protein. In the DnaK–DnaJ–substrate complex, the substrate is transferred to the hydrophobic cleft located on the Hsp70 SBD. The cleft is solvent-accessible in the ATP state of the chaperone. By combined action of DnaJ and bound substrate, the Hsp70 hydrolyzes ATP. This leads to a large-scale conformational change in which the substrate becomes more tightly bound. EM-structural analysis of an Hsp70 bound to a full-length protein client confirms that the binding takes place through the SBD [43]. Nucleotide exchange factors (NEF; GrpE in the case of *E. coli*) help the Hsp70 to acquire ATP, reversing the conformational change, and reducing the affinity of the Hsp70 for the substrate, after which it is released. This cycle constitutes the so-called "holdase" and release function of the Hsp70 (see Fig. 2). This function is utilized to transport un/mis-folded proteins between organelles or to protect the un/mis-folded proteins from aggregation until more favorable folding conditions exist [44].

In addition to the holdase function, the Hsp70's main function is to help in the protein (re)folding process. Hsp70s such as DnaK, in the presence of DnaJ, GrpE, and ATP, can refold heat-denatured luciferase [45], polymerase [46], and resolubilize protein aggregates [47]. In fact, in the eukaryotic cytosol, Hsp70s are the predominant protein (re)folding machine, handling more substrates (20% of the proteome) [48] than the eukaryotic GroEL analog TRiC (7% of the proteome) [49]. Protein refolding must involve an active unfolding step of the substrate [4, 50, 51]. Possible mechanisms are (1) that Brownian motion of the chaperone loosens the bound misfolded protein, in a process called entropic pulling [52], (2) that misfolded proteins are inherently unstable and will transiently expose additional hydrophobic sequences which are trapped by additional DnaJ and/or DnaK, leading to progressive unfolding in a multi-molecular complex, (3) a combination of (1) and (2) [47], and (4) that the closure of the Hsp70 lid upon binding to the client is a molecular wedge to alter the conformation of the bound substrate [43]. Unfolded protein is subsequently released by action of the NEF, after which it can spontaneously refold. Especially in the refolding function (Hsp70 as "foldase" actually, better, "un-foldase") timing and kinetics must be critical to success.

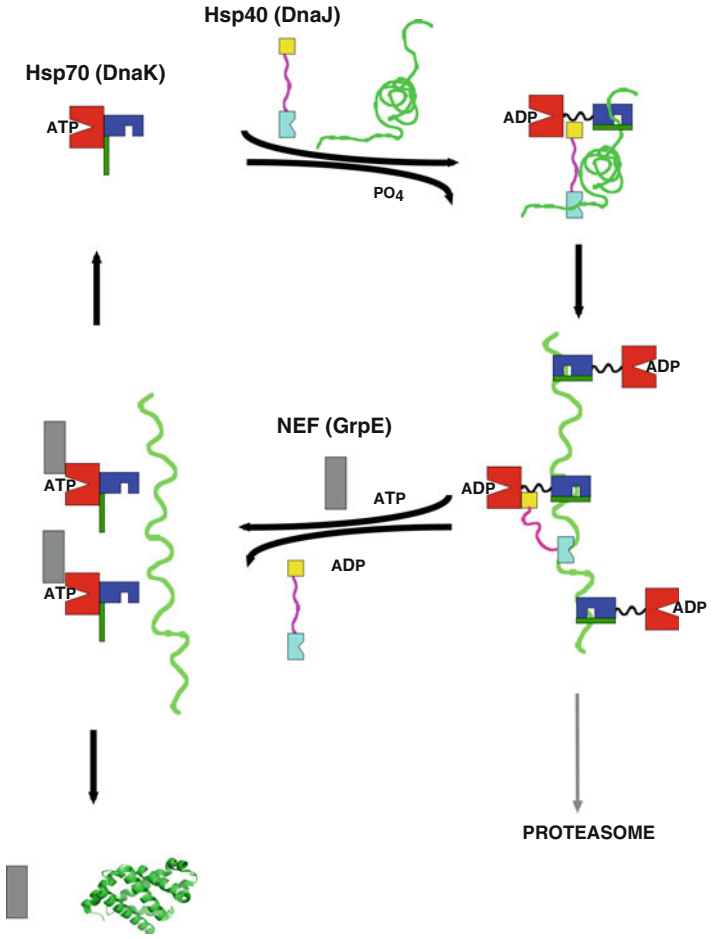

Fig. 2 The Hsp70 functional cycle as an unfoldase. DnaK NBD is in *red*, SBD is in *blue*, LID is in *dark green*. DnaJ J-domain is in *yellow*, DnaJ SBD is in *cyan*, DnaJ GF-region is in *pink*. Substrate (client) is in *green*. NEF is in *gray*. The oligomeric complex with several Hsp70s and Hsp40s is unproven. Successful cycles result in unfolded protein that can spontaneously refold. Unsuccessful cycles result in protein degradation by the proteasome

4 Allostery and Structures of Hsp70

Hsp70s are allosteric proteins in which ATP binding at the NBD causes substrate release at the SBD, and in which substrate binding causes hydrolysis of ATP, and in which hydrolysis of ATP enhances substrate binding. In the ADP state substrate binding is tight, while in the ATP state, the substrate binding affinity is reduced by one to two orders of magnitude [53–55] (depending on substrate and species; see Table 2). As the distance between the nucleotide binding cleft and substrate binding cleft is more than 50 Å, the clefts must communicate indirectly by allostery.

Table 2 Thermodynamics and kinetics of DnaK substrate-binding allostery

σ^{32}(132–144) binding to DnaK [54]				CALLQSRLLLSAPRRAAA binding to DnaK [55]		
	K_D	k_{on}	k_{off}	K_D	k_{on}	k_{off}
ATP	1.8 μM	1.3×10^6 M^{-1} s^{-1}	2.31 s^{-1}	2.2 μM	4.5×10^5 M^{-1} s^{-1}	1.8 s^{-1}
ADP	78 nM	1.17×10^4 M^{-1} s^{-1}	0.001 s^{-1}	63 nM	9.3×10^3 M^{-1} s^{-1}	0.004 s^{-1}
Ratio ATP/ADP	23	109	2,566	35	48	450
ΔΔG or ΔΔG‡	1.9 kCal M^{-1}	2.8 kCal M^{-1}	4.7 kCal M^{-1}	2.1 kCal M^{-1}	2.3 kCal M^{-1}	3.7 kCal M^{-1}

Our discussion here will focus mostly on allosterics as observed in DnaK, the Hsp70 of bacteria *E. coli*. This is because much of the early Hsp70 work was carried out for DnaK and also because the majority of the recent structural information on allostery has been collected on DnaK. We are, as of this writing, not aware of any structural/kinetic/thermodynamic findings that are fundamentally different for the mammalian Hsp70s. The latter differ from DnaK *E. coli* mostly in the utilization of different co-chaperones.

The difference in the affinity for substrate in the case of DnaK-ATP and DnaK-ADP corresponds to a free energy of allostery of only 2 kcal/mol (see Table 2) [53–55]. This is less energy than is contained in a typical H-bond. However, the substrate off-rate is different by three orders of magnitude between the ADP and ATP state, which corresponds to a respectable change of 4–5 kcal/mol in the free-energy of the dissociation activation barrier.

DnaK's allostery can be measured in a number of ways. In vitro assays include stimulation of ATP-hydrolysis upon substrate binding [56], which can be monitored by detecting the release of ortho-phosphate by γ^{32}P radio-isotope assays [57], colorimetric assays [58], or ^{31}P NMR spectroscopy [59]. In addition, substrate binding at the SBD may be monitored by change in the emission maximum of the intrinsic fluorescence of Trp102 of DnaK [60], which is located in the subdomain IB of the NBD [61]. The fluorescence change can hence be used to monitor allosteric communication. Furthermore, the quintessential substrate release upon ATP binding can be monitored by a decrease in the fluorescence anisotropy of fluoroscein-labeled substrate peptides [62]. Nucleotide and substrate binding result in global changes in the DnaK molecule. The linker between NBD and SBD is more easily cleaved in the ADP state than in the ATP state [61]. Also, amide proton exchange in the SBD is different in ADP and ATP states [63]. Finally, extensive chemical shift changes of the NMR lines of the NBD occur when peptide becomes bound to the SBD [64], and, conversely, the NMR spectrum of the SBD changes upon ADP/ATP exchange in the NBD [65].

In vivo assays of Hsp70 functionality include evaluation of capability of cells to survive heat shock [66], and, for DnaK in particular, its ability to stimulate lambda-phage growth in *E. coli* [67]. A stringent test is the refolding of mutated or heat-denatured luciferase, which will only occur in the presence of ATP and co-chaperones of the DnaJ and NEF class [45]. Recently, suspicions that all of these functional/biophysical assays may not perfectly correlate with each other have been put forth [68, 69].

Much about allosteric mechanisms of proteins can usually be learned from the comparison of the structures of different allosteric states of the proteins. The classical example is the comparison of the crystal structures of oxyhemoglobin and deoxyhemoglobin. The conformational differences seen provided strong clues about the allosteric mechanism, which was eventually verified with biochemical and genetic experiments. A similar structural analysis has been a longstanding goal in the Hsp70 field. While structures for isolated NBDs [37, 70–72], SBDs [37, 73, 74], and LID [37, 75] were published almost two decades ago, structural biology techniques have only recently captured a few constructs that contain both NBD and SBD

[38, 64, 76, 77]. For the Hsp70s, at least four allosteric states should be compared: NBD(ATP)-SBD(apo), NBD(ATP)-SBD(sub), NBD(ADP)-SBD(sub), and NBD (ADP)-SBD(apo). In addition, one can add NBD(apo)-SBD(apo) and NBD(apo)-SBD(sub). However, nucleotide-free NBD can exist only transiently during the ADP → ATP exchange and should not be considered to be a physiologically relevant state. Nevertheless, biochemical evidence suggests that its properties are not unlike the ADP-bound state [61]. ATP hydrolysis in the NBD(ATP)-SBD(sub) state is relatively rapid (0.05–0.5 s^{-1}) [56]. Consequently, the lifetime of this state is too short for structural studies. This leaves three other relevant states to be studied. The NBD(ADP)-SBD(sub) state is completely stable in the absence of NEFs and so is the NBD(ADP)-SBD(apo) state. The NBD(ATP)-SBD(apo) state is stable enough for most biophysical experiments (ATP hydrolysis rate is 5×10^{-4} s^{-1}) [56], but not for NMR or X-ray structure determination.

In addition to these fundamental considerations, there are technical problems. The Hsp70s tend to aggregate in both ADP and ATP states, especially when the SBD cleft is unoccupied, and the NBD-SBD linker is very susceptible to proteolytic cleavage. These properties hamper both NMR and X-ray studies. Hsp70s are "large" for NMR, precluding high-resolution structure determinations to be made (except for the isolated SBD [73, 78]). As multi-domain proteins of dynamical nature, Hsp70s also are a challenge for X-ray crystallography, both in crystallization and in the effect of packing on the relative (sub)domain positions in the crystal.

Because of these technical issues, only one of the four allosterically relevant structures is available to date: it is the NBD(ADP)-SBD(sub) state, determined in solution from a *combined* analysis of X-ray structural data of the subdomains, with NMR residual dipolar couplings which delineate the relative domain orientations. The structure was obtained for wt-DnaK in the presence of ADP, phosphate, and the peptide NRLLLTG ($K_D = 5$ μM) [38]. In this structure, the LID domain is docked to the SBD, but the SBD-LID unit moves rather unrestricted with respect to the NBD [38] as can be seen from the NMR intensity data presented in Fig. 3. Using ^{15}N NMR relaxation data, it was established that the dynamics of the SBD is consistent with motion in a cone of 70° opening angle with respect to the NBD, and that the time scale of the motion is shorter than 1 ns. The study substantiated earlier NMR studies that noted that the NBD and SBD behave as independent units in the ADP state [65, 79]. So the NMR data from two groups show that there is no stable communication between NBD and SBD in the ADP state. Hence, one expects that the two domains must interact in the ATP state.

By itself this is an interesting finding: conventional understanding is that allostery involves (at least) two well-defined states, in which the interaction free energy between the allosterically-coupled units differs. Possibly this outlook may be derived from the fact that virtually all structural studies of allosteric systems have been studied by crystallography, a method which can only characterize well-defined states. Possibly, allostery involving dynamic, "non-communicating" states is widespread, but has gone undetected. Alternatively, we observe here a primitive form of allostery. It must be simpler evolutionarily to develop interface

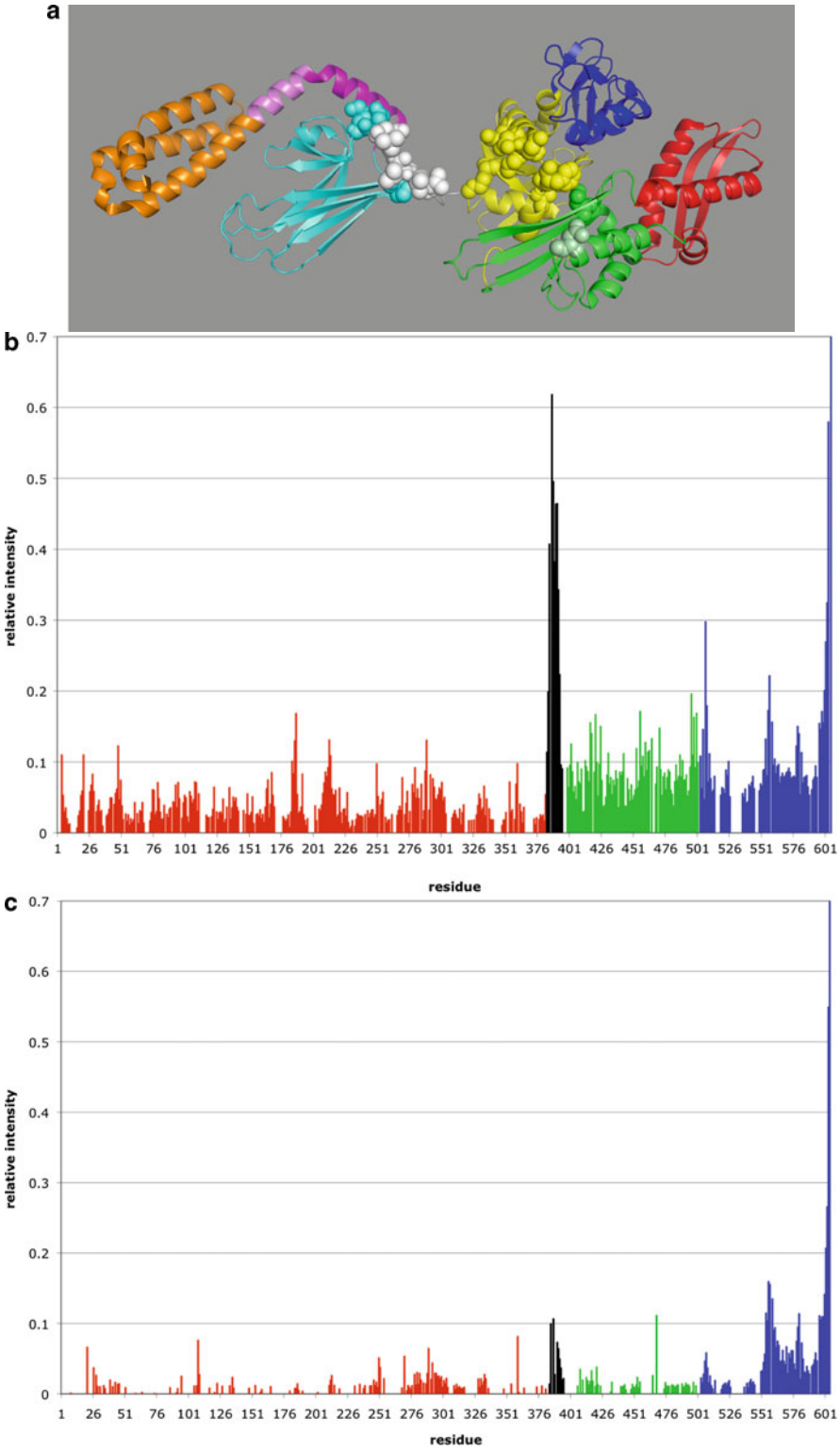
a
b
relative intensity
0.7
0.6
0.5
0.4
0.3
0.2
0.1
0
1 26 51 76 101 126 151 176 201 226 251 276 301 326 351 376 401 426 451 476 501 526 551 576 601
residue
c
relative intensity
0.7
0.6
0.5
0.4
0.3
0.2
0.1
0
1 26 51 76 101 126 151 176 201 226 251 276 301 326 351 376 401 426 451 476 501 526 551 576 601
residue

complementarity in only one instead of two allosteric states. Hsp70s, which are some of the most ancient proteins [5], may have conserved this mechanism.

The following other two-domain structures are available, but neither of these contains wild-type proteins.

First, an NMR solution conformation is available for a truncated construct of the DnaK of *Thermos thermophilus*, in the ADP state, but without bound substrate [64]. This protein, an NBD(ADP)-SBD(apo) state construct, is missing the complete alpha-helical LID domain. It does not show relative domain motions. Its overall domain alignment is within experimental uncertainty, identical to that of wt-DnaK-*E. coli* NBD(ADP)-SBD(sub). Whether the lack of inter-domain motion is caused by the lack of the LID, the lack of substrate, or the fact that the experimental data were recorded at 55 °C, a temperature well below the temperature of optimal activity of *T. thermophilus* (65–80 °C), is currently unknown.

Second, a crystal structure of a two-domain construct of bovine Hsc70 truncated at residue 554 was reported [76]. The C-terminus binds to the substrate-binding cleft. In this construct, NBD and SBD were found to interact. However, the mutations E213A and D214A, which were essential to the crystallization process, are found to be on the interface between NBD and SBD (see Fig. 4). It is likely that these aggressive mutations are the cause of the observed hydrophobic packing between NBD and SBD. We believe that the crystal structure for this Hsc70 triple-mutant [76] is artifactual.

Third, a crystal structure of DnaK(1–509) from *Geobacillus kaustophilus* bound in the ADP state was reported [77]. The construct is missing the alpha-helical LID domain. The crystal contains dimers, in which the SBD of one monomer binds to the NBD-SBD linker of the other monomer. While this is not likely to be a physiologically relevant state, the structure does show that the NBD and SBD are significantly separated from each other, in agreement with NMR solution structure of wt-DnaK in the ADP state [38].

Fourth, a crystal structure of SSE1, an Hsp110 from *S. cerevisiae*, has appeared [80]. Hsp110s are homologous to Hsp70s, and bind ATP stably without hydrolyzing it. Despite the fact that the Hsp110 crystal structure is a dimer mediated by LID–LID interactions, the NBD-SBD interface may be representative of the Hsp70 ATP state.

Fig. 3 (**a**) The relative orientation of the SBD (*left*) and NBD (*right*) for DnaK(1–605) in the ADP – NRLLLTG state in solution [38]. NBD domain IA: *yellow*, IB: *blue*, IIA: *green*, IIB: *red*, linker: *white*, beta domain: *cyan*, LID-helix-A: *magenta*, LID-helix-B: *pink*, Lid: *orange*. Residues rendered in space fill are important for the NBD-SBD allosteric communication as determined by mutagenesis studies from several other workers as discussed in the text. (**b**) Dynamical properties of the ADP-NRLLLTG state of the DnaK backbone as determined from cross-peak intensity of HNCO NMR data [38]. High intensity indicates high mobility, low intensity indicates low mobility. Colors: NBD: *red*, Linker: *black*, SBD: *green*, LID: *blue*. (**c**) Dynamical properties of the ATP-APO state of the DnaK (1–605)(T199A/V436F) backbone as determined from cross-peak intensity of HNCO NMR data. High intensity indicates high mobility, low intensity indicates low mobility. Colors: NBD: *red*, Linker: *black*, SBD: *green*, LID: *blue* (Bertelsen and Zuiderweg, unpublished)

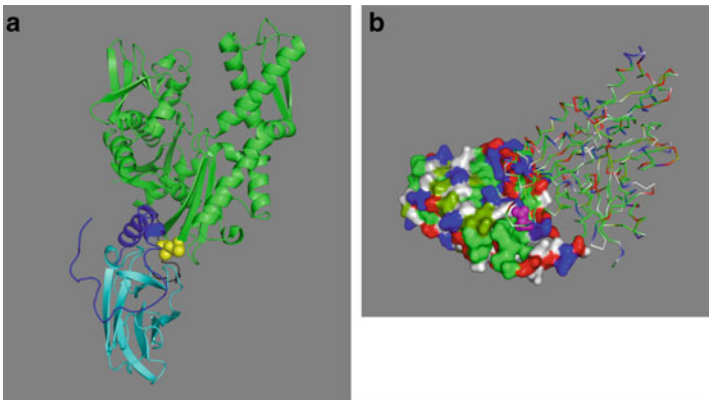

Fig. 4 A crystal structure of human Hsc70 Δ(555–646) E213A/D214A [76]. (**a**) *Left*, overall docking. *Green*: SBD, *cyan*: SBD-beta; *blue* LID; *black* NBD-SBD linker. A213 and A214 are *yellow*. (**b**) *Right*, docking of the NBD (ribbon) on the SBD/LID/Linker (surface). The linker is at the *bottom*. Color coding: *green*: apolar, *red*: negative, *blue*: positive, *white*: polar, *mud-green*: Thr + Tyr. The mutations A213 and A214 on the NBD are in *pink* and interact directly with a hydrophobic SBD surface

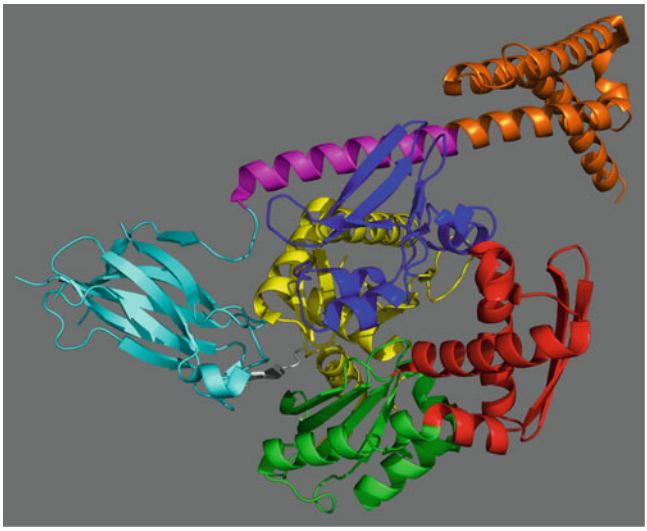

Fig. 5 A crystal structure of Hsp110 of *S. cervisea* [80] Orientation and color coding is as in Fig. 3a. (NBD domain IA: *yellow*, IB: *blue*, IIA: *green*, IIB: *red*, linker: *white*, beta domain: *cyan*, LID-helix-A: *magenta*, LID-helix-B: *pink*, Lid: *orange*)

It is depicted in Fig. 5. The structure shows a docked NBD and SBD, in agreement with the expectation for the ATP state of Hsp70. The linker is engaged as an additional strand of the two-stranded beta sheet in NBD subdomain IIA. This docking would explain the extensive solution NMR chemical shift changes upon ATP/ADP exchange

seen for residues in these strands [64, 65, 81, 82]. The LID in Hsp110 has moved away from the SBD and is docked against subdomain IB. This docking would explain the fact that the fluorescence of Trp102 in subdomain IB of DnaK is affected by the ATP-ADP conformational change, but not in the absence of the LID [61]. Despite all these expected features, there is still doubt as to the validity of Hsp110 as a model for the Hsp70 ATP-apo state. In particular, the lack of homology for the linker (see Table 1) is of great concern. The linker plays a key role in the allosteric function of the Hsp70s (see below). The linker sequence VLLLD, strongly conserved between Hsp70 members, is DIHPY in Hsp110. On the one hand, the differences in linker are quite to be expected as they would explain why Hsp110 is locked in the ATP state; on the other hand, one questions whether the observed docking in Hsp110 can be representative of the presumed docking in the Hsp70s since the differences in physico-chemical properties of the linker residues are so large.

A recent NMR contribution from the Gierasch group [83] is weighing in on this discussion. They observe chemical shift changes in the two-stranded beta sheet in NBD subdomain IIA between DnaK NBD constructs with and without the linker, but only in the ATP state. While no actual structure determination was carried out, these results were interpreted to reflect that, only in the ATP state, the linker may form an additional strand of the two-stranded beta sheet in NBD subdomain IIA. Hence, this study supports the claim that the crystal structure of SSE1 [80] may indeed be a model for the ATP state of the Hsp70 chaperones.

Nevertheless, as of this writing, this leaves us with only one reliable structure for a full-length and authentic Hsp70: it is the solution structure of wt-DnaK in the NBD(ADP)-SBD(sub)state in which no communication between NBD and SBD takes place [38, 65]. Hence all understanding of the allosteric mechanism for Hsp70s has to be derived from either structural studies of the individual domains and their changes upon ligand binding or biochemical/biophysical studies of the full-length proteins without direct structural insights.

Fortunately, many such studies are available, and will be reviewed below.

5 Global Characteristics of the Allosteric Change

The γ-OH of Hsc70 active-site residue T13 (T11 in DnaK *E. coli* numbering) forms a hydrogen bond with an oxygen of the ATP γ-phosphate. This hydrogen bond is one of the few direct links between the nucleotide and NBD subdomain IA (see above). Mutation of T13 to valine did not affect the efficiency of ATP hydrolysis, but completely abrogated the allosteric communication between NBD and SBD [84]. The mutation T13S was allosterically active [84] and structural studies revealed that its γ-OH took the position of the γ-OH of Thr. These findings underscore the importance of this single hydrogen bond for the allosteric mechanism. Possibly it is the key linkage signaling the nucleotide state to subdomain IA, which, in turn, propagates the signal to the SBD (see below). However, the

mechanism is probably more complicated: mutation of Hsc70 residue K71 (K70 in *E. coli* numbering), the only ATP-contact residue derived from subdomain IB (and essential for ATP hydrolysis [32]) also abrogating the ATP-induced conformational change (as determined by SAXS) [32]. Hsc70 point-mutations E175S, D199S, and D206S also bind ATP and also impair the ability of ATP to induce a conformational change [32] (E171, D194, and D201 in *E. coli* numbering). All of these residues are involved in coordinating Na^+ or K^+ ions, which in turn neutralize the ATP γ-phosphate. The mutation E543K on the LID can "rescue" the ATP-induced transition for E175S/E543K, D199S/E543K, and D206S/E543K. E543 (D540 *E. coli*) forms a salt-bridge with R469 (R467 *E. coli*), stabilizing the LID-closed, ADP state. It is likely that the E543K mutation destabilizes the ADP state, facilitating the ATP-induction of the LID-open state. Hence, it is likely that the mutations E175S, D199S, and D206S attenuate, but do not eliminate, allosteric communication. The γ-OH of T204 (T199 *E. coli*) was initially thought to be a candidate for the nucleophile attacking the ATP. However, its mutation to Ala yielded a protein that could still turn over ATP (albeit less efficiently), and in which allostery was intact [85]. The same mutation in *E. coli* (T199A) had the same phenotype [61, 86]. A rather rigorous mutation in the DnaK substrate binding cleft, V436F, retained significant substrate binding capability, and retained allostery [61, 87, 88].

Some representative mutations of surface residues that yield Hsp70 constructs that still can hydrolyze ATP and bind substrate, but which lack allosteric coupling, are Y145A, N147A, and D148A [86]; P143G and R151A [89]; K155D and R167D [35]. Mutagenesis of most residues of the NBD-SBD linker leads to loss of allosteric communication [35, 90]. On the SBD, mutations K414I [62] and P419A [91, 92] eliminate allostery. N415G and D326V attenuate allostery [93]. All mentioned positions are listed in DnaK *E. coli* numbering and are shown in Fig. 3. The NBD surface mutations all occur in subdomain IA facing the SBD in the solution structure except for D326V on subdomain IIB, rendered in a different shade of green in Fig. 3. The SBD mutations occur on the solvent exposed loops that face the NBD in the solution structure of the ADP state. These areas are potentially in contact in the ATP state. Recent work showed that these areas have been subject to co-evolutionary mutagenesis [93], further bolstering the observation that they could be in contact in the ATP allosteric state.

SAXS experiments showed considerable changes in overall molecular shape between the ATP and ADP allosteric states of Hsc70 [94, 95]. The ADP state is extended and monomeric, while the ATP state has a more globular shape. However, the SAXS experiments on the ATP state should be critically viewed, considering that this state has a strong tendency to aggregate at the concentrations needed for SAXS.

Both hydrogen exchange and limited proteolytic digestion studies of DnaK show that ATP binding stabilizes the NBD, while simultaneously destabilizing most of the SBD [61, 63].

Gierasch and coworkers observed that the TROSY NMR spectra of the isolated NBD and isolated SBD superimposed well on the TROSY NMR spectrum for DnaK in the ADP state, but not for DnaK in the ATP state [65, 79]. This data suggested that

NBD and SBD do not interact in the ADP state, but do interact in the ATP state. The former observation was fully confirmed in the solution structure of DnaK in the ADP state (see Fig. 3). In this figure the intensities of the HNCO cross peaks are plotted as well [38]. Larger peaks indicate greater mobility of the associated amino acid residues. Clearly, the SBD and LID domains have equal mobilities, while the NBD domain has a different mobility. NBD-SBD domain docking in the ATP state is confirmed with NMR mobility data on a DnaK construct in the ATP state as shown in Fig. 3c. This figure also shows that part, but not all, of the LID is undocked in the ATP state.

Extensive domain dynamics has also been observed in FRET studies of the yeast Scc1 DnaK homolog [96]. Fluorophores attached to NBD position 341 (318 in DnaK *E. coli* count) and SBD position 448 (425) are closer to each other in the presence of ATP than in the presence of ADP. The distance distribution is much wider for the ADP state than the ATP state, in agreement with the relative mobility of the NBD and SBD in that state. Fluorophores attached to SBD position 448 (425) and LID position 590 (564) are closer to each other in the presence of ADP than in the presence of ATP, showing that the LID undocks in the latter state. Again, the distance distribution is wider for the ADP state than the ATP state, suggesting that the LID can also undock in the ADP state.

As deduced from the following observations, the determinants for the allosteric communication appear to be solely embedded in the NDB and the beta domain of the SBD and the NBD-SBD linker. The LID domain, which certainly has to move away from the beta domain to allow substrate binding and release, does not directly drive the allostery. Mutant DnaK in which the complete LID was deleted (1–507) showed wild-type activity in the ATP-hydrolysis and ligand fluorescence assays (see Fig. 6) [74]. When the severely truncated DnaK(1–507) was expressed in a DnaK-deficient strain, it still supported significant bacteriophage growth [74]. It is unknown, but unlikely, that this construct is also functional in protein refolding, given the pivotal role of the LID in regulating the kinetics of substrate binding and release [97–104].

Other workers have also shown that other "lidless" constructs retain considerable allostery [97, 98, 101–104]. It seems prudent to conclude that the conformational changes of the LID domain are a result rather than a cause of the Hsp70 allostery. However, comparisons of the kinetics of ligand binding and hydrolysis between wild-type and constructs lacking the LID showed that the LID domain affects the kinetics of substrate binding and release in a dramatic fashion [97, 98, 101–104]. Fine control of substrate binding and release kinetics must be essential to the protein refolding machinery – maybe even more so than thermodynamics (see below).

6 The Key Role of the NBD-SBD Linker

The ten-residue linker between NBD and SBD is mostly hydrophobic and strongly conserved between Hsp70s (see Table 1). This linker is more exposed in the ADP than in the ATP state according to proteolysis assays [105] and hydrogen exchange

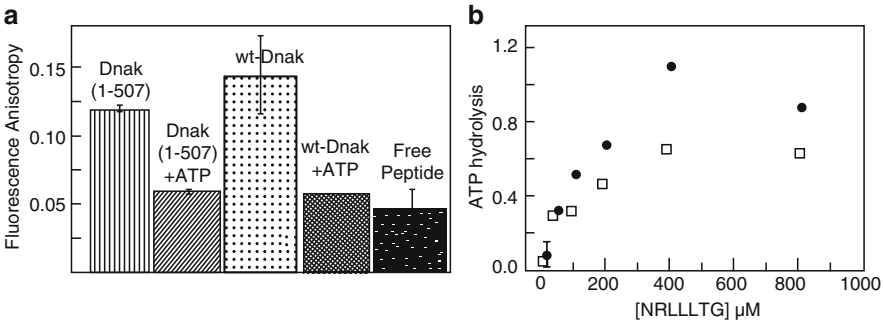

Fig. 6 In vitro studies of DnaK(1–507) allosteric function. (**a**) ATP-induced release of peptide F-APPY in DnaK(1–507) measured by fluorescence anisotropy. The *first bar* represents the anisotropy value for peptide bound to 1.1 mM DnaK(1–507). The *second bar* represents the anisotropy value 5 min after addition of 0.44 mM ATP. The *third and fourth bars* represent the values for wt-DnaK under comparable conditions, and the *last bar* indicates the anisotropy value of free peptide. *Error bars* reflect the standard deviation from a mean of three measurements. (**b**) Peptide stimulation of ATPase activity of DnaK(1–507) (P) and wt-DnaK (m). As DnaK (1–507) is titrated with the peptide NRLLLTG, the ATPase activity is stimulated in a manner similar to that of wt-DnaK. The hydrolysis rate is reported as moles of ATP hydrolyzed per minute per mole of DnaK(1–507) or wt-DnaK. The *error bar* on the first point reflects the standard deviation from a mean of three measurements and is valid for both assays. From [74]

experiments [63]. This is fully confirmed with the NMR dynamics data in Fig. 3: in the ADP state the linker is very mobile, while the linker in the ADP state is docked. Combined with the knowledge that mutations in the linker are detrimental to the allosteric coupling [90, 106], these results imply a significant role for the linker in allosteric signal transduction between the NBD and SBD.

Mayer and co-workers were the first to observe that the ATP-hydrolysis rate by the isolated NBD of DnaK(2–393) was 41-fold faster than that of DnaK(2–385) [35]. The difference between these constructs lies in the presence or absence of the linker sequence ^{386}VKDVLLLD^{393}. As such, the mere presence of the linker in this truncated construct mimicked, partially, the hallmark allosteric stimulatory effect of substrate binding in the context of the wild-type protein. The mutation D393A abolished the enhancement. This demonstrated that the linker itself is necessary and sufficient for allosteric control of the NBD. Together with the observations that mutations of the hydrophobic residues interfere with allostery [90, 106], and with the observation that mutation of D388 did not interfere with allostery [35], the essential part of the linker is demarcated as ^{389}VLLLD^{393}.

The effect of the presence of linker on the ATP hydrolysis rate was independently observed by Gierasch and co-workers, who found that DnaK(1–392) was a 13-fold more efficient enzyme than DnaK(1–388) [65]. These workers used NMR investigations to characterize the differences between the NBD constructs. The domains in the ADP state revealed major chemical shift differences for about 50 residues between DnaK(1–392) and DnaK(1–388). In addition, the four C-terminal residues of DnaK(1–388) were seen to be mobile. Significantly, the C-terminus of

DnaK(1–392) was not mobile, indicating that the linker is docked in this construct. Using selective labeling experiments, it was possible to show that L177 and I373 in the IA-IIA hydrophobic cleft undergo large chemical shift changes between the two constructs. The sidechain of L177 is part of the surface of the IA-IIA hydrophobic cleft. I373 is completely buried but packed against L177. It was suggested that the shifts of these residues indicate that the linker binds in this cleft. Recent work strongly suggests that DnaK residues 215–220, which form the edge strand of the beta sheet in subdomain IIA, interact with the NBD-SBD linker in the ATP state but not in the ADP state [83]. There is some indication that the linker forms an extra strand of the beta sheet. Very likely this interaction is crucial to the propagation of the allosteric signal from the NBD to the SBD [80].

Mayer and coworkers set out to identify the electrostatic partner for linker residue D393 on the NBD surface [35]. Mutagenesis of likely candidate residues R151, K155, and R167 in the IA-IIA cleft showed those to be important for the regulation of allostery in the context of the full molecule. However, charge reversal mutations of these residues in the context of DnaK(2–393) exacerbated the ATP hydrolysis enhancement effect instead of abolishing it. So, it is unlikely that D393 interacts with these positive residues in DnaK(2–393). This leaves one with the suspicion that the interaction of the linker in the context of the isolated NBD could be different to that in the full protein. In this context it is interesting to note that crystal structures of linker-extended Hsc70 NBD constructs did not show electron density for the linker, and their three-dimensional structures were identical to those of constructs without the linker [107].

7 Allosteric Changes in the NBD

The linker interacts differently with the NBD in the ATP state compared to in the ADP state [35, 65, 83] . Hence, one expects differences for the structures of the NBD in these different states. Remarkably, only very small differences were observed between the conformation of the (isolated) NBD by X-ray crystallography in the presence of a variety of nucleotide analogs (see Fig. 7), making it difficult to explain *why* the linker docks in one state but not the other. However, NMR spectra showed distinct differences in chemical shifts between the ADP and ATP states in Hsc70 [81] and in DnaK [82, 108], especially in the groove between NBD subdomains IA and IIA. This strongly suggests that conformational changes also occur in solution for the isolated NBD (Fig. 7).

Since these conformational changes are not observed in the crystal, the energy difference between them is likely to be small, which is in agreement with the overall characteristics of the Hsp70s as described at the outset. The solution-detected differences reveal much of the workings of the Hsp70 allosteric machine. With the modern NMR method of residual dipolar couplings, relative domain orientation can be determined in solution, even though detailed changes and translations cannot [109]. Using these methods it was possible to detect up to 9° rotation between the

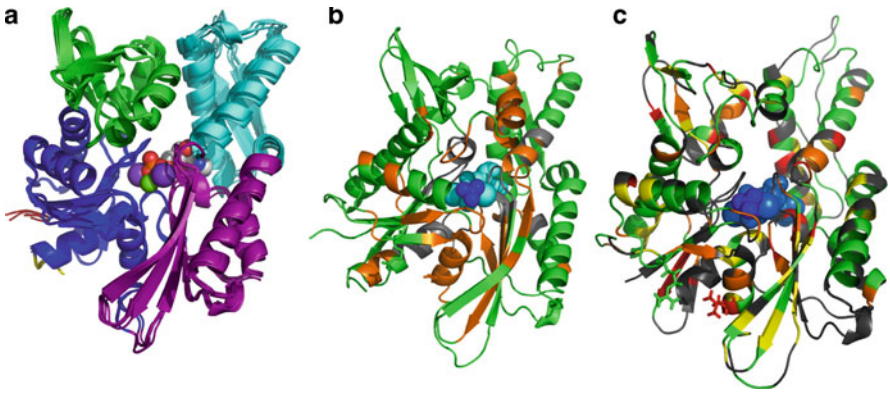

Fig. 7 (**a**) Superposition of five crystal structures for bovine Hsc70 NBD: wt-APO (2QW9.pdb), wt-ADP.PO_4 (3HSC.pdb and 2QWL.pdb), wt-ADP.VO_4 (2QWM.pdb) and K71M-ATP (1KAX.pdb). The N-terminus is in *red*, the C-terminus is in *yellow*. (**b**) ^{15}N-^{1}H chemical shift differences between the ATP and ADP.Pi conformation of Hsc-70-NBD. *Orange*: significant shift, *green*: no shift, *gray*: not known. (**c**) ^{15}N-^{1}H chemical shift differences between the AMPPNP and ADP.Pi conformation of TTh-NBD. *Red*: large shifts; *orange*: medium shifts; *yellow*: small shifts; *green*: no shift; *gray*: not known. ADP is in *light blue*, PO_4^{3-} in *dark blue*

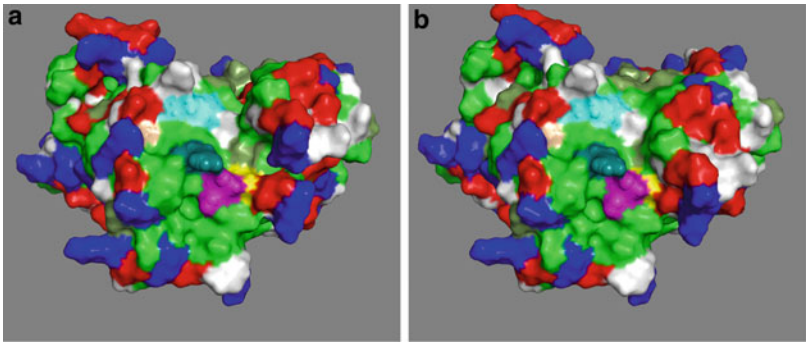

Fig. 8 The SBD's view of the IA/IIA interface of DnaK-TTh. (**a**) *Left*: in the ADP state. (**b**) *Right*: in the AMPPNP state [82]. Color coding: hydrophobics, *green*; positive, *blue*; negative, *red*; polar, *white*. The C-terminus (residue 372) is *magenta*. Residue L174 (L177 in DnaK *E. coli*) in *yellow*, residue R148 (R151 in *E. coli*) in *cyan*, residue A152 (K155 in *E. coli*) sand, residue R164 (R167 in *E. coli*) in teal

different subdomains for the isolated NBD of DnaK *T. thermophilus* (TTh) when comparing the ADP and AMPPNP states [82]. In particular, the hydrophobic cleft between subdomains IA and IIA is different between the AMPPNP state and the ADP state. The structure calculations suggest that the groove is narrow and deep in the ATP state and broad and shallow in the ADP state (see Fig. 8). However, the calculations are based on rotations of entire subdomains without translational information, and the accuracy of the presented structural models is very limited.

Nevertheless, the rotation of subdomain IIA relatively to subdomain IA is real (with 97% significance), which will obviously affect the details of the groove between the subdomains. Figure 8 also shows the locations of the different relevant residues discussed in the previous paragraph.

The NMR data show that the nucleotide-binding cleft is "closed" in the ATP state and is "open" in the ADP state. These studies suggest that the crystal structures of the isolated NBD all correspond to the "closed" ATP state, irrespective of the bound ligand.

Different orientations of the NBD subdomains have also been observed, by crystallography, for NBDs complexed with different nucleotide exchange factors [71, 110–113]. These studies show that subdomain rotations are also possible in the crystal. Similar changes have been seen for actin and hexokinase, which show considerable structural homology with the Hsp70 NBD [31]. The nucleotide binding cleft is more open in the Hsp70-NEF-complexes. The open state of Hsc70 with an NEF in the crystal resembles the ADP state of DnaK *TTh* without an NEF in solution [82]. This would suggest that the NEF captures and stabilizes the more open ADP state.

What local changes could allow these global rotations? The sugar-ribose moiety and alpha-phosphate of ATP is exclusively in contact with subdomains IIA and IIB. Only the beta and gamma phosphates contact subdomain IA (hydrogen bonds with Thr14 NH and Thr13 NH, respectively), and form the only link between lobes II and I (from inspection of the structure of Hsc70-K71M, with bound ATP). Breakage of the gamma-phosphate, as has occurred in the ADP state of the protein, may therefore weaken the link between the lobes, allowing for (dynamic) rearrangement of the relative positions of these lobes. In this way, the state of the deeply buried nucleotide can be signaled to the surface of the NBD by (dynamic) subdomain rotations. The rotations are probably responsible for the change in access to the hydrophobic cleft between IA and IIA as was described above.

Mayer and co-workers have discovered an interesting mutation R151K in DnaK, which abolishes all allosteric communication [63, 89]. R151K is located in subdomain IA and its sidechain is partially exposed to the groove between subdomains IA and IIA. In the Hsc70 crystal structure the guanidinium group of the homologous R151 is within hydrogen bond distance of the carbonyl oxygen of P143. P143, in turn, stabilizes E175, which protrudes into the nucleotide-binding pocket (see Fig. 9). The authors hypothesize that the NBD nucleotide state affects this network reversely, possibly by a proline *cis-trans* isomerization and a more extensive conformational change in segments 139–163 and 165–177, which flank the IA-IIA cleft. This change then leads to a change in the linker docking. Substrate binding hypothetically reverts all of these conformational changes, in particular in Pro143 (*cis-trans* isomerization) and E171, thereby bringing the catalytic K70 with its coordinated water molecule into the ideal position for ATP gamma-phosphate cleavage.

Whether this hypothetical mechanism actually contributes to nucleotide-cleft signaling awaits investigation of the mutant R151K by structural analysis.

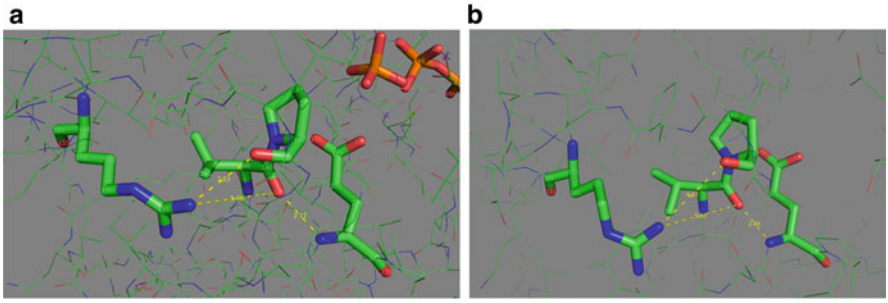

Fig. 9 (**a**) *Left*: the hypothetical "proline switch" in Hsc70 ADP.Pi. (**b**) *Right*: the hypothetical "proline switch" in DnaK-*E. coli* without nucleotide. Following [89]

8 Allosteric Changes in the SBD

The SBD has been extensively investigated (see Fig. 10). Its topology is unique in the PDB [36]. A crystal structure of an SBD-LID construct of DnaK showed that the substrate-binding cleft is lined with hydrophobic residues to which a hydrophobic substrate (NRLLLTG) binds [37]. The cleft shows one particularly deep pocket that accommodates the sidechain of Leu4 of the substrate. The backbone of the substrate is stabilized by H-bonds to the main chain of the SDB. The SBD is a rather "flat" molecule, with the binding cleft spanning the short axis. The cleft just about covers the seven-residue substrate; hence it is believed that an Hsp70 can in principle bind to stretches of seven exposed residues in un- or misfolded proteins.

In the substrate-bound form, the LID is closed. LID helices A and B (the rising and horizontal helices in Fig. 10) are stabilized by a combination of hydrophobic and charge interactions, while the part that covers the cleft has exclusively charge–charge interactions [37, 115]. Recent NMR data [38] confirms that, in solution and with NBD present, the complete LID domain is docked to the beta basket in the ADP state and when substrate is present (also see Fig. 3b). Figure 3c shows that the latter section of the lid un-docks when the ligand is absent with the NBD the ATP state. This result confirms, with direct data, the long-standing belief that the lid must come off the cleft for binding or release of substrate protein.

Interestingly, the NMR dynamics data in Fig. 3c suggest that the release does not engage the entire LID, and confirms an early hypothesis based on slight structural differences at exactly this hinge point between different molecules in the crystallographic unit cell [37]. However, it disagrees with our earlier hypotheses that the entire LID can come off, which was based on observations of displacements of the entire helix with respect to the beta domain for different SBD constructs [73, 78]. Muga and co-workers [115] found that mutations at the N-terminus of the horizontal helix destabilize the ADP but not the ATP state, also suggesting that the entire helix comes off in the ATP state. Other data also suggest that the entire helix B can come off: for DnaK it is well known that W102 fluorescence changes upon binding of ATP [100, 116]. The change is compatible with a reduction in solvent exposure of this residue, which is located in NBD subdomain IB. This change in fluorescence is lost

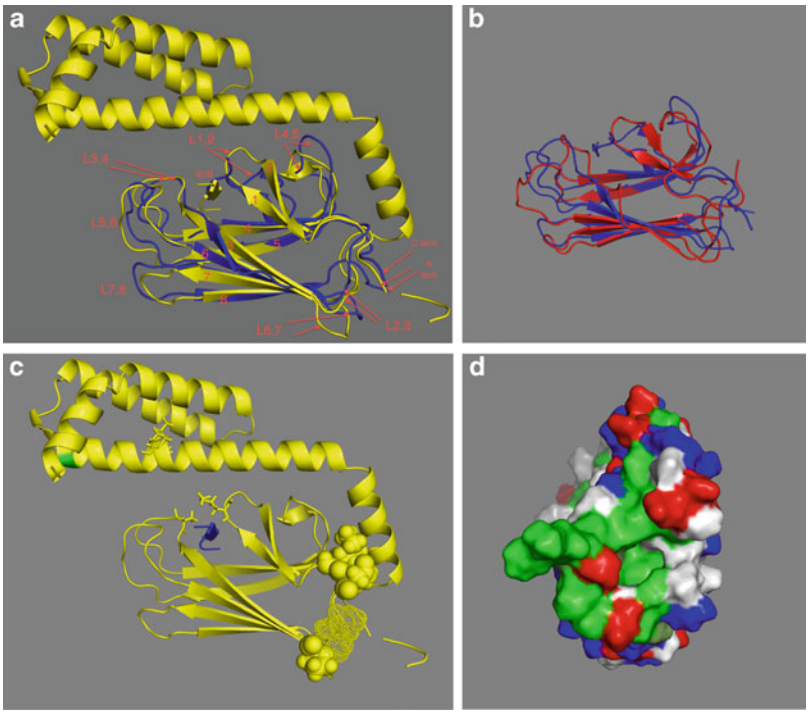

Fig. 10 (**a**) Comparison of *E. coli* DnaK(389–605)-NRLLLTG (*yellow* [37]) with DnaK (393–507)-NRLLLTG (*blue* [114]), with nomenclature following [37]. (**b**) Comparison of DnaK (393–507)-NRLLLTG (*blue* [114]) with DnaK(393–507).apo (*red* [74]) (**c**) DnaK(389–605)-NRLLLTG. The ligand is in *blue*. Residue 552 is in *green*. L542Y, L543E on the LID are in *sticks*. K414, N415 and P419 are in *space fill*, T417 and I418 are in *dots*. (**d**) The N-terminal "face" of DnaK(389–605)-NRLLLTG. Phobics are in *green*, positives in *blue*, negatives in *red*, polars *white*. The structure protruding at 3 o'clock is the residual NBD-SBD linker, with Asp393 (*red*) close to the SBD core

upon removal of the entire LID as in truncation DnaK(1–507) [99, 117]. Nevertheless, allosteric communication, as judged by peptide-release stimulation by ATP and ATP hydrolysis stimulation by peptide, is still fully functional in DnaK(1–507) [74, 117]. This suggested that, in the ATP-apo state, the LID may directly collide with NBD subdomain IB. It is of interest to note that the crystal structure of Hsp110, potentially a model for Hsp70 in the ATP state, shows direct contact between the LID helix and subdomain IA [80]. Muga and co-workers [117] also found that the W102 fluorescence change remains in DnaK(1–537), suggesting that N-terminus of helix B, must come off to allow changing interaction with subdomain IA.

The following results may shed light on this conundrum. Using EPR spinlabels and cysteine cross linking, Mayer et al. [68] show that the LID can hinge at residue 515 (between helix A and B) and also at residue 530 (in helix B, close to the binding cleft, see in Fig. 3c) but that these different modes depend on the nature of the substrate offered: binding/release of entire proteins requires the first mode.

Gierasch and co-workers [79] used NMR to study the DnaK(387–552, L542Y, L543E), a construct containing both beta basket and helices A and B of the LID. The mutations were made to avoid self-binding of the truncated lid [78] (see Fig. 10c). Changes in chemical shifts of DnaK(387–552, L542Y, L543E) upon titration of NRLLLTG were small, and localized around the substrate cleft. The pattern of hydrogen exchange protection with and without bound substrate were largely the same, although the overall stability of the domain was slightly enhanced by the substrate. Analysis of NOEs and hydrogen bonding confirmed that DnaK (387–552, L542Y, L543E) showed very little and certainly no widespread conformational change upon ligand binding. These studies present a question: if no changes occur in the SBD structure upon substrate binding, how does substrate binding get transmitted to the NBD?

The above results are at variance with the results of an earlier NMR investigation, in which DnaK(393–507), containing only the beta basket, was investigated [74]. As stated above, lidless DnaK(1–507) is functional protein in vitro and, at least partially, in vivo. Hence, one expects that the basket alone should display allosteric effects. The properties of substrate-bound and substrate free basket differed greatly. In the presence of substrate, the basket was rigid (confirmed with ^{15}N relaxation measurements; L. Wang and E. Zuiderweg, unpublished), and the solution structure was identical to the corresponding region of the crystal structure of substrate-bound DnaK(389–605) [114] (Fig. 10a). In contrast, unliganded basket is a dynamic molecule which fluctuates between different conformations on the milli/microsecond time scale [74]. All resonances for loops 3, 4, 5, and 6 (see Fig. 10a for nomenclature) were broadened away beyond detection, suggesting a dynamical collapse, or melting, of part of the substrate binding cleft. Less, but still significant, broadening was observed for Q424, V425, F426, and S427, which in the liganded structure form the latter half of beta strand 3. It was concluded that the latter part of this strand is dynamically disordered in the apo state. Broadening was also observed for the amide protons T417 and I418 in loop 2,3 which are quite remote from the cleft, and which "face" the NBD in the structure in Fig. 3. Hence, the NMR data show a conformational/dynamical linkage between events in the substrate binding cleft and loop 2,3.

^{15}N relaxation studies on the basket showed that the rotational correlation time of the domain decreases from 12 to 7 ns upon binding of NRLLLTG (L. Wang and E. Zuiderweg, unpublished). Such a change in rotational correlation time is compatible with a change from dimer to monomer. Dilution experiments suggest that $K_{\text{dimer}} < 1$ μM. Ligand-linked monomerization could explain why the substrate NRLLLTG binds with considerably lower apparent affinity (600 μM) [74] than to wild-type protein (5 μM) [37], even though the structure of the bound complex is similar to the wt structure (Fig. 10). Isotope-edited NOE experiments on mixed ^{15}N-^{14}N labeled protein preparations showed NOEs between the ^{15}N and ^{14}N labeled proteins, confirming the existence of a dimer for the APO state of the basket (S. Stevens and E. Zuiderweg, unpublished). Significantly, the inter-monomer NOEs suggested that dimerization was not mediated by the substrate-binding pocket. In contrast, a few inter-monomer NOEs to residues in the

hydrophobic "face" of the SBD shown in Fig. 10d and at the beta sheet at the "bottom" were observed, suggesting that the dimerization interaction may take place at these locations. Despite this unnatural (?) dimerization of the isolated beta basket, the fact remains that substrate binding/release causes major changes in its properties. This is in line with expectations for an allosteric protein. Apparently, a protein–protein interaction interface is only exposed in the apo state but not in the substrate-bound state. This is quite reminiscent of the fact that the SBD interacts with NBD in the apo state but not in the substrate-bound state. It is tempting to speculate that the unnatural dimerization of the isolated SBD without LID fortuitously mimics the interaction of the SBD with the NBD. However, if such is true, why was this unnatural dimerization not seen for the beta domain extended with helices A and B [79]?

Perhaps the combined results point to the following mechanism. (1) In the SBD apo-state, there exists a patch which is poised for protein–protein interactions. (2) Without NBD and LID, the patch interacts to form unnatural homo-dimers. (3) *Without* NBD but *with* LID, the patch is covered by the LID. (4) With LID and with NBD, the NBD displaces the LID from the patch because NBD has a high affinity for that patch (or NBD-SBD linker; see below).

This hypothesis would suggest that the internal substrate-binding allostery of isolated SBD is different from the internal substrate-binding allostery of the SBD in presence of NBD. The following supports such a view. While the isolated DnaK (387–552, L542Y, L543E) showed little difference in hydrogen exchange rates between apo and substrate-bound states [79], widespread changes in amide proton protection were seen upon ADP/ATP exchange for the SBD in the two-domain construct DnaK(1–552, L542Y, L543E) [65]. In particular, Thr 420 and V436 are more exposed in the ATP state, whereas H422 is protected in that state.

These findings correspond closely to those of Mayer and co-workers [118] who mapped the differences in amide proton exchange of DnaK(T199A) between ADP and ATP state using proteolysis and mass spectrometry. ATP hydrolysis in DnaK (T199A) is greatly reduced, but allosteric communication with the SBD is maintained. Figure 11 shows that the SBD is dramatically destabilized in the ATP/apo state, just as was found for the isolated beta basket without substrate [74]. Noteworthy is that stretch 413–437 and the edge strand of the lower beta sheet become more exposed in the ATP state. The former area contains the mutation sites K414I [62] and P419A [91, 92] and N415G [93] which abolish or attenuate allosteric communications. Regretfully the resolution is not high enough to distinguish the loop from the strand. Substrate binding significantly reduced amide proton exchange in the beta domain, especially on the longer time scale. Regretfully, again, the resolution is too low to disclose whether global rigidification or just local rigidification around the peptide binding cleft occurs.

New amide proton exchange experiments [118] for wt-DnaK in the ATP-APO state show a gradient of deprotection towards loops 3,4 and 5,6 closely corresponding to the melting of the substrate-binding cleft in the isolated beta basket in the APO state [74].

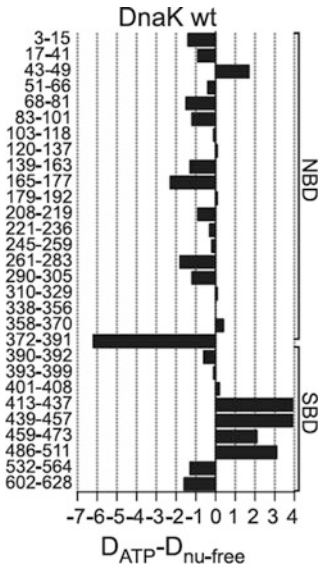

Fig. 11 Differences in amide-proton exchange for *E. coli* DnaK in the ATP and ADP state. Positive numbers indicate less protection in the ATP state. From [63]

Taken together, there is sufficient evidence from several sources to suggest that widespread conformational/dynamical change takes place in the SBD upon ligand binding and/or ATP/ADP binding. The results obtained for the construct containing both beta basket and helices A and B of the LID, which did not show such changes [79], appear surprising in this context, but do help in underlining the subtleties of NBD/beta/LID/linker/substrate interactions, and the need for further investigations.

9 Where Does the SBD Interact with the NBD in the ATP State?

As discussed above, we do not believe that any valid Hsp70 structures in which NBD and SBD dock have yet been described. In the previous section we hypothesized that a hydrophobic "face" of the SBD, may interact with the NBD in the NBD(ATP)-SBD(Apo) state.

There have been suggestions that the hydrophobic linker may interact with a hydrophobic patch that "faces" the NBD as seen in Fig. 10b [37, 78]. In this way, the NBD and SBD never interact directly – interaction is mediated by the linker from both sides. Presence of a hydrophobic site in the corresponding SBD area has been confirmed: NMR signals for L392, L397, and A413 disappeared while V394, T395, L484, and L507 weakened in the NMR spectrum of DnaK(386–561) due to interaction with a hydrophobic peptide labeled with paramagnetic label [78]. Significantly, L392 is part of the linker, while A413 is next to the mutation sites K414I [62] and N415G [93] that affect allostery. It was also noted that LID helix A is docked to the same hydrophobic patch [78]. Perhaps the NBD-SBD linker can displace the LID in the ATP form.

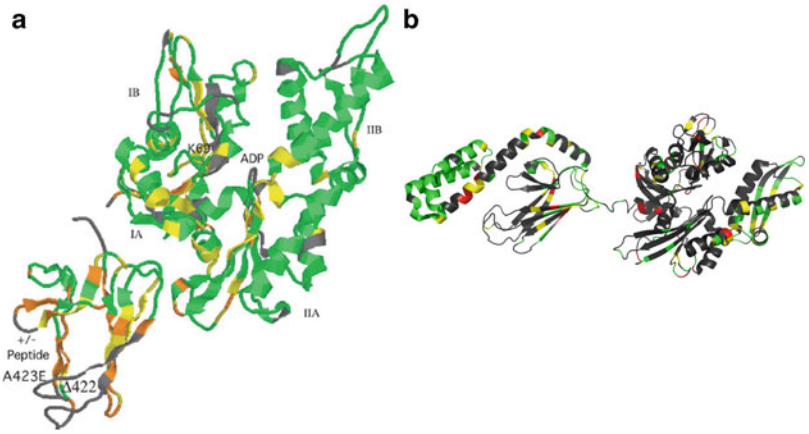

Fig. 12 Chemical shifts changes and two-domain allostery. (**a**) Chemical shift changes between the ADP-apo and ADP-NRLLLTG state in DnaK *T. Thermophilus* (1–501) From [64]. (**b**) Chemical shift changes between ADP-apo DnaK E. coli (1–605) and ATP-apo DnaK *E. coli* (1–605) (T199A/V436F) (Bertelsen and Zuiderweg, unpublished)

Table 3 Sequence homology of Hsp110 *S. cerv.* vs Hsc70 *H. sapiens*

	Identity (%)	Homology (%)		Identity (%)	Homology (%)
IA	35	61			
IB	30	55	Linker	12	32
IIA	44	76	Beta	10	20
IIB	42	67	LID	16	31
NBD	35	60	ALL	25	44

The precise mechanism by which the substrate binding is signaled to the loop that contains K414?, P419A and N415G is unknown. Perhaps the intrinsic flexibility of this loop as seen in substrate-free SBD [63, 74] allows a captured fit [119] of the NBD-SBD linker, while the rigidification of the entire domain upon ligand binding is sufficient to interfere with this process. This mechanism would be related to allostery by dynamic change alone, predicted by Cooper and Dryden [120], and experimentally confirmed by NMR studies for several systems [121–126].

On the other hand, there are also indications that beta strands 3, 6, 7, and 8 of the SBD are involved in contact: residues in these strands show dramatic chemical shift changes between the NBD(ADP)-SBD(apo) state and the NBD(ADP)-SBD(sub) state of *TTh* DnaK(1–501) [64] (see Fig. 12a). Similarly, chemical shifts in these strands were identified when comparing the NMR spectrum of DnaK(1–605) in the NBD(ADP)-SBD(sub) state with that of DnaK(1–605) T99A V436F in the NBD (ATP)-SBD(apo) states (Fig. 12b).

Surprisingly, no changes were observed in either of these cases for the residues in the Loop 2,3 facing the NBD, which contains all the mutation sites mentioned. Clearly, more work is still needed to understand fully the complete allosteric pathway in the SBD of the Hsp70s.

10 Relevance of Hsp70 Allostery

Structural and dynamical properties for the two "end-point" allosteric states are listed in Table 4. Some, but not all aspects of this table can be represented in a cartoon as shown in Fig. 13. It is truly amazing that so many differences exist, while the free energy of allostery is only a few kcal/mol as judged from the difference in substrate binding energy between these states (Table 2). The real conundrum, however, is that the corresponding small difference in substrate binding constants (~2 μM for the ATP state and 70 nM for the ADP state; see Table 1) can only discriminate between ligands in the concentration range of 200 nM: ten times more concentrated substrates would remain bound even to the ATP state, while ten times less concentrated substrates would not even bind to the ADP state. Such a concentration limitation seems awkward for a molecular machine that needs to refold a variety of proteins over a wide concentration range.

Maybe one should look at this differently. Classically, the argument is that the free energy of ATP hydrolysis is needed to unfold the misfolded proteins; in this view, little of the ATP hydrolysis energy remains to effect conformational changes in the Hsp70 themselves. However, ATP's free energy may not be (directly) needed for the unfolding task: the gain in hydrophobic interaction between substrate and SBD should at least partially compensate for the loss of energy associated with the loss of aggregation. In turn, the loss of the interaction energy upon release of the substrate is at least partially regained in the hydrophobic docking of NBD and SBD in the ATP state. In this view, considerable fractions of the 7–14 kcal/mol of ATP hydrolysis energy (depending on conditions) may be used to break the NBD-SBD interface and be the cause of the major conformational changes seen. In this view, substrate binding to the ADP state does not need to be tighter than substrate binding to the ATP state. This hypothesis also explains how substrate could efficiently bind to the low-affinity open ATP state at the start of the chaperone cycle, while it is efficiently released from this same state at the end of the cycle. Indeed, all that is needed is that the chaperone is brought into contact with the substrate (with help of DnaJ, see below) and retains its substrate long enough to allow unfolding by Brownian motion, referred to as "entropic pulling" [52], with the possible assistance of multiple copies of DnaK or DnaJ (transiently) binding to the same target (see Fig. 2 and [127] and see below). Opening of the substrate binding cleft at the end of the cycle is then sufficient to let the unfolded protein diffuse away. In this sense, the "thermodynamic" allostery would play only a minor role in the functional cycle. One may quantify this as a mixed thermodynamic/kinetic mechanism as follows. Substrate binding occurs with the high association rates of the DnaK-ATP state and dissociates with the slow dissociation rate of the ADP state. Such a *non-equilibrium* K_D is in the order of 1 nM (k_{on}(DnaK-ATP) ~ 1×10^6 M^{-1} s^{-1}, k_{off}(DnaK-ADP) ~ 0.001 s^{-1}; see Table 1). This "affinity" is high enough to bind even low-abundant proteins. Upon nucleotide exchange the K_D reverts to that of the ATP state, i.e., it increases 1,000-fold. Potentially, NEFs can even compete for the bound substrate (see below), further reducing effective substrate affinity. Viewed in this mixed thermodynamic/kinetic way, the Hsp70s could successfully operate on substrates in a concentration range between 1 and 1,000 nM.

Table 4 Summary of allosteric changes

	Nucleotide binding cleft	IA-IIA cleft	NBD dynamics	Linker	SBD	SBD dynamics	LID
NBD(ATP)-SBD(apo)	Closed	Open	Rigid	Docked	Docked	Millisecond/microsecond time scale[a]	Released
NBD(ADP)-SBD(sub)	Open	Closed	Second/decisecond time scale[b]	Mobile	Not docked	Rigid	Docked

[a]Extensive NMR line broadening observed
[b]Multiple NMR peaks in slow exchange observed

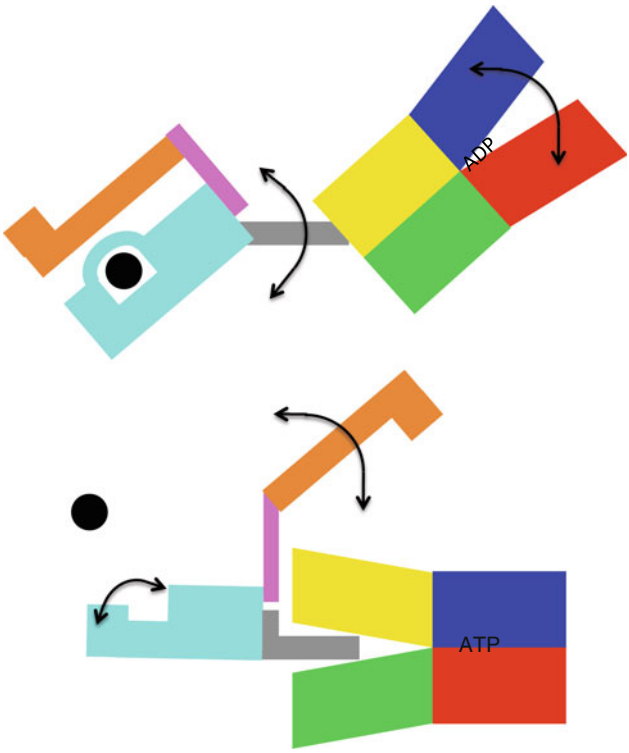

Fig. 13 Cartoon representation of the allosteric changes between the ADP.sub state (*top*) and ATP-apo state (*bottom*). Color coding is (as in Fig. 1): NBD subdomain IA, *yellow*; IB, *blue*; IIA, *green*; IIB, *red*; linker, *gray*; beta domain, *cyan*; LID-helix-A, *magenta*; Lid, *orange*. Relative domain orientations of NBD, SBD and LID in the top cartoon are representative of reality (see Fig. 1). The relative domain orientations of those domains in the bottom cartoon are based on the hypotheses reviewed herein. Also see Table 4

The kinetics of the Hsp70 chaperone system is complex. It involves substrate on-off processes, nucleotide on-off processes, lid opening and closing, ATP hydrolysis, and conformational changes. In addition, co-factors such as DnaJ and GrpE bind and release and affect the rates mentioned above. It is not the purpose of this chapter to review the large body of literature on this subject. We note that Witt and coworkers [97, 101, 128–131], Christen and co-workers [132–135], and Bukau and co-workers [56, 61, 136] have contributed much to this field.

11 The Role of the NEFs in Allostery

Nucleotide exchange factors enhance the exchange of ADP for ATP up to 1,000-fold [133, 137]. At the present time, four very different NEFs have been co-crystallized with Hsp70 NBDs: GrpE [71], BAG-1 [110], BAG-2 [138],

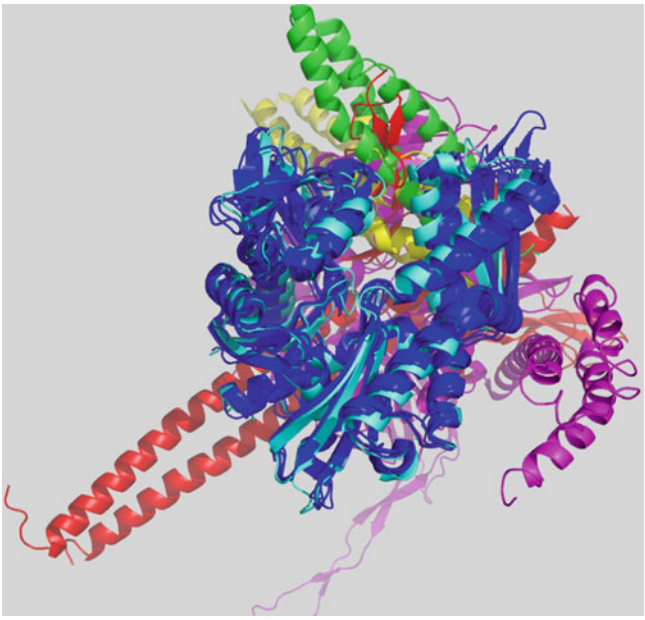

Fig. 14 NBD-NEF complexes. The NBDs were superposed and all colored *blue*. GrpE (1DKG) in *red*; Hsp110 (3C7N) in *magenta*, BAG-1 (1HX1) in *green*; BAG-2 (3CQX) in *yellow*. The NBD of Hsc70 without NEF (3HSC) is shown in *cyan*

Hsp110 [80, 139] (see Fig. 14). A partial structure is available for exchange factor HSPBP [111, 140]. While the binding interfaces between the factors and the Hsp70 are vastly different, all Hsp70 NBDs in the different complexes have in common that the nucleotide binding cleft is opened wider than in isolated Hsp70 NBD crystal structures. These observations clearly account for enhanced access and egress of the nucleotide. Initially the NEFs were thought to open actively the NBD cleft in an induced-fit mechanism [71, 110]. However, in light of the wide variety of NEFs which all achieve the same effect, it is more reasonable to assume that NEFS capture (transient) opening fluctuations of the NBD. This is in line with the recent solution NMR data that show that the nucleotide binding cleft in the isolated NBD in the ADP state is considerably more widely open than in the ATP state [82]. Such a "captured fit" would also provide a mechanism for GrpE to interact exclusively with the (dynamic) ADP-like state, and not with the static closed ATP state; the latter would be a wasteful and undesirable interaction.

The bacterial NEF, GrpE, has a remarkable structure. It is a hammer-like dimer, which (also in solution [141]) interacts with a monomeric Hsp70. The interaction of the NBD occurs mostly by the head of the hammer. Upon inspection of the crystal structure of the complex, the authors suggested [71] that the shaft might interact with the SBD (which was absent in the complex). Interestingly, the simple exercise of superposing the common NBD in the crystal structure of DnaK(NBD)-GrpE [71] with the solution structure of wt-DnaK in the ADP-sub form [38] places the end of

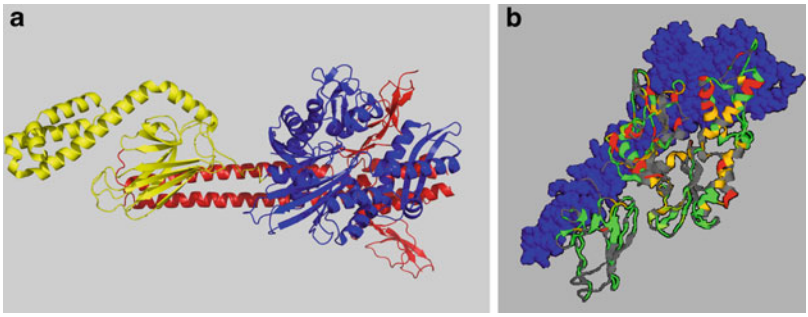

Fig. 15 Hypothetical GrpE-DnaK complexes. (**a**) Model of a functional *E. coli* DnaK-GrpE complex based on the structures of DnaK ADP.NRLLTG (2KHO) and DnaK-NBD + GrpE 40–197 (1DKG.pdb) in which the NBDs were superposed. GrpE is in *red*. The GrpE N-terminus (residue 40) is at the *left*. (**b**) Chemical shifts occurring on DnaK *T. Thermophilus* (1–501) upon addition of GrpE *T. Thermophilus*. Model composed as in Fig. 15a (Deep and Zuiderweg, unpublished)

the GRPE shaft in immediate vicinity of the SBD cleft (see Fig. 15a). GrpE residues 1–37, which would extend even further towards the SBD cleft, are not visible in the crystal. It is intriguing that a hydrophobic sequence ^{17}Ile-Ile-Met^{19} exists in this otherwise hydrophilic area of GrpE. We speculate that these residues may be responsible for the demonstrated competition of the GrpE N-terminus with substrate [142]. Indeed, the affinity of Hsp70 for substrate in the ATP state is actually not that much lower than that in the ADP state (see Table 2) and assistance to remove substrate from the ATP state is likely necessary.

Our lab has collected chemical shift evidence showing interaction of the GrpE shaft with the SBD for a two-domain construct of DnaK *T. thermophilus* and the N-terminus of GrpE *T. thermophilus* (S. Deep and E.R.P. Zuiderweg, unpublished; see Fig. 15b). Folding/unfolding transitions in the GrpE N-terminus have been shown to act as a thermostat for the DnaK activity [141]. This hypothesis does not seem valid for eukaryotes. BAG proteins, the NEFs of Hsc70, do have extended, likely unfolded areas at the N-terminus, but, according to the crystal structure of the Hsc70–BAG1 domain complex, this area would not be in the vicinity of the SBD.

12 The Role of DnaJ in Allostery

The human genome codes for 50 J-proteins are subdivided into three classes: DnaJA, DnaJB, and DnaJC (see Table 5). The J-proteins are also referred to as Hsp40. Like Hsp70s, DnaJs also bind to stretches of exposed hydrophobic residues in client proteins. DnaJ *E. coli* [143] and DnaK *E. coli* [144] substrate specificities are similar, and both prefer hydrophobic sequences. However, DnaJ can also bind to synthetic D-amino acid peptides [145]. This strongly suggests that DnaJ does not make hydrogen bonds in the peptide backbone of its client, but instead interacts

Table 5 DnaJ nomenclature and structure. The sequence numbers are for YdJ1 (yeast)

Type	Example	J-domain (1–70)	GF region (71–110)	SBD(116–145 and 208–255)	Zn-domain (146–206)	GM region	SBD-duplicate (260–340)	Dimer helix (350–360)	Extended Tail (370–409)
DNAJA (Type I)	DnaJ E. coli Ydj1 yeast HDJ-2 human	Present	Present	Present	Present		Present	Present	Present
DNAJB (Type II)	HDJ-1 human Sis1 yeast	Present	Present	Present		Present	Present	Present	
DNAJC (Type III)	pyJ polio virus	Present							

mainly with hydrophobic sidechains and is more forgiving in the substrate's local structure.

The most commonly [45] but not universally [42] held view is that DnaJ apportions the clients to DnaK which is in the ATP-apo state with an open SBD. After or during the process of client transfer, DnaK hydrolyzes ATP and assumes the ADP-(sub) state. However, the chaperone activity of DnaK in luciferase refolding was maximal at a DnaJ concentration 100-fold lower [45, 46] than the typical K_D for DnaJ substrate interaction (around 1 μM, see above). Moreover, it had been discovered that the maximum enhancement of DnaK ATPase activity by DnaJ occurs at a different molecular to that for optimal refolding [117]. These facts suggest a more "catalytic" and transient role for DnaJ once DnaK has acquired client (see below).

The four human type A J-proteins show strong homology to *E. coli* DnaJ, and show a complex domain topology (see Table 5 and Fig. 17). They contain an N-terminal J-domain, a glycine/phenylalanine-rich region, a Zn-finger domain, a substrate binding domain, a copy of a substrate binding domain, and a variable C-terminal domain. The N-terminal 73-residue J-domain is the most conserved, and its structure has been determined for several homologs in the context of truncation mutants (1–70 to 1–108) [100, 129, 130]. The structure is essentially an anti-parallel two-helix bundle with two small adjacent helical elements. (see Fig. 16). The J-domain alone is sufficient to stimulate ATPase activity of Hsp70 [125]. There is a conserved HPD sequence located in a flexible loop connecting the main helices II and III. Mutations in the HPD motif and in positively charged residues of helix II of the J domain abolish functional interactions with partner Hsp70s [126, 150]. This identified the J-domain as the domain that recognizes DnaK. Indeed, it was found by NMR that J(1–75) interacts with wt-DnaK in the ADP state and also with the isolated DnaK NBD [151]. The K_D for this interaction was around 10 μM. This K_D value may seem to be too weak to be of physiological relevance. However, as will be outlined below, DnaJ is a "poly-dentate" ligand for DnaK to which the J-domain interaction is only one of the determinants. Helix II of DnaJ is most involved in the interaction with DnaK [151]. This helix contains several conserved Lys and Arg residues, which are sensitive to mutation [126, 150]. It has therefore been suggested that the interaction between the J-domain and DnaK is electrostatic in nature [151]. Only small perturbations were found for the NMR chemical shifts of the HPD loop [151]. Recent studies of our group confirmed these findings – there are *no* changes for the NMR chemical shifts of the HPD loop [152]. These results are surprising in the light of the mutational sensitivity of these residues [126, 150]. Mutations in the HPD loop do not affect the interaction with the ADP state, but do strongly diminish the affinity of the J-domain for ATP state of DnaK [153]. At present it is not known if the HPD loop is directly involved in the interaction with DnaK, or if it stabilizes the interaction-competent J-domain conformation.

A crystal structure is available for YDJ1(110–337) [147], a DNAJA protein. It shows two highly homologous beta domains. Substrate is bound in a hydrophobic surface cleft of the first beta domain. The Zn-Cys domain is seen to be an insert in the first beta domain (see Fig. 17a).

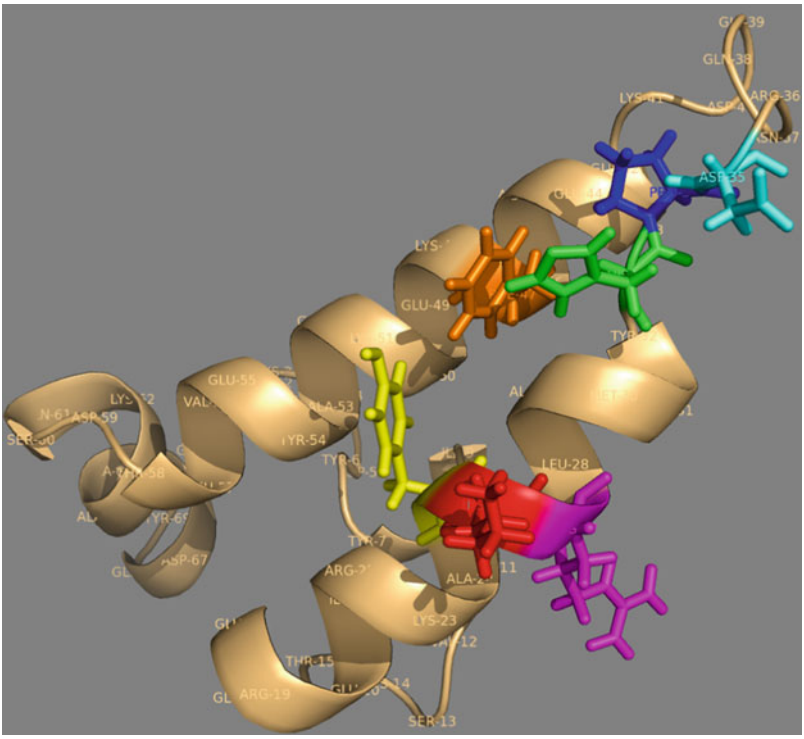

Fig. 16 The solution structure of *E. coli* DnaJ(2–76) in context of DnaJ(2–108) (1XBL) [148]. The mutationally sensitive [149] residues Y25 (*yellow*), K26 (*red*), R26 (*magenta*), H33 (*green*), P34 (*blue*), D35 (*cyan*), and F47 (*orange*) are highlighted

The Gly/Phe-rich region (residues 75–110) connects the J-domain with the C-terminal domains. A NMR solution investigation of DnaJ(1–108) [154] showed that the GF-region was dynamic and disordered. The role of the Gly/Phe-rich region is likely to allow flexibility in relative position and orientation of the J-recognition domain and DnaJ's substrate binding domain. The flexibility would increase the probability of substrate transfer to the DnaK SBD (or simultaneous substrate binding) while the J-domain binds to the DnaK NBD.

However, why does the G-F domain contain phenylalanines and not serines or threonines? In addition, why do G-F region mutations of DnaJ residues ^{90}FSDIFGDVFG^{100} affect DnaJ function [155]? Recently our lab obtained evidence [152] that the G-F domain interacts with DnaK's SBD substrate binding cleft in the absence of other substrate. That is, the G-F region is the second site of a DnaJ poly-dentate interaction. Figure 18 illustrates our way of thinking about the J-K complex. Because of the multi-dentate interactions many binding modes are possible, while the individual interaction determinants are not of very high affinity (1–10 μM).

Gross and co-workers carried out SPR measurements with different DnaK and DnaJ constructs. The key findings of their first paper in this area [156] are that DnaK

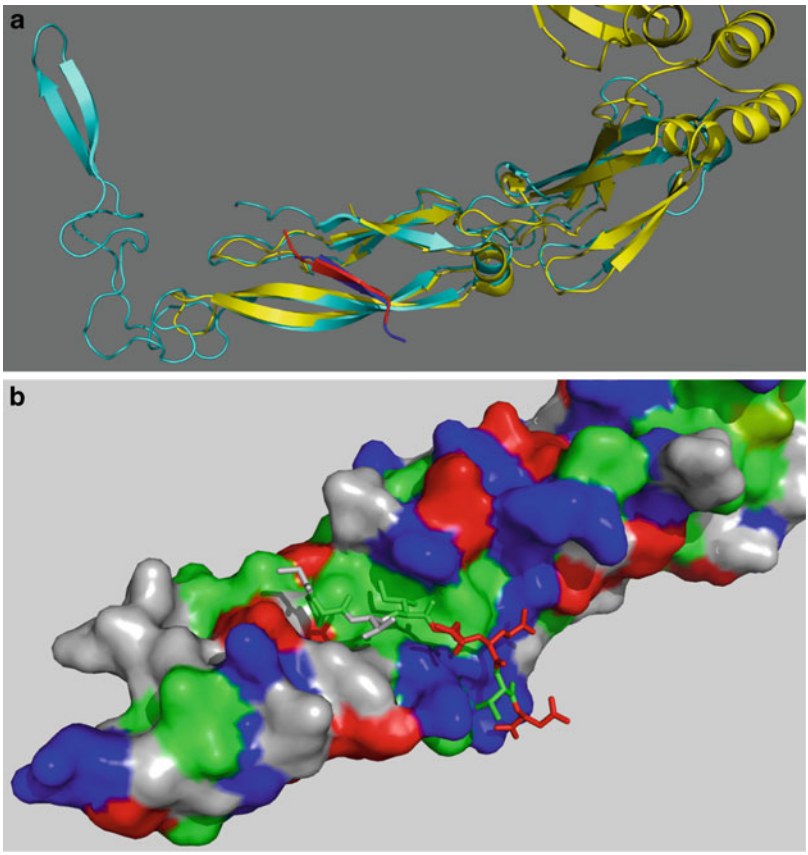

Fig. 17 (**a**) Overlay of a crystal structure of the peptide-binding and dimerization domain of human HDJ1 [146] in *yellow*, with that of yeast YDJ1 [147], in *cyan*. The HDJ1 substrate (GPTIEEVD) is in *red*, the YDJ1 substrate (GWLYEIS) is in *blue*. The CA positions in the SBD (193–240 and 205–252 for HDJ1 and YDJ1, respectively) were superposed. YDJ1's Zn domain is at the left, HDJ1's dimerization helices are at the *right* (the latter were deleted in the crystallization construct of YDJ1). (**b**) Detail of the hydrophobic cleft of HDJ1, composed of residues M183, I185, L204, I206, F220, I235, and F237 and ligand GPTIEEVD

mutants in the NBD (R167A, N170A, and T173D) and the SBD (G400D and G539D) individually reduce the wt-DnaJ binding tenfold. Since these mutations occur on both NBD and SBD, this result also shows that DnaJ is poly-dentate. The key findings of their other work in this area [157] are that DnaJ does not bind to DnaK(1–403) (NBD) or to DnaK(386–638) (SBD). Similarly, while DnaJ(1–108) binds almost as well as wt-DnaJ, DnaJ(1–75) does not bind. In the context of SPR, this indicates $K_D > 1$ μM. These results are consistent with the fact that the binding constants of the individual determinants are indeed around 10 μM. Others have shown bidentate interaction as well. Laufen et al. [106] showed that DnaJ was inefficient in stimulation of ATP hydrolysis by a DnaK mutant with defects in substrate binding, suggesting synergistic action of DnaJ and substrate. Others [158, 159] show that DnaJ(1–70) required either the GF-rich region or a peptide substrate provided in trans to strongly enhance DnaK's

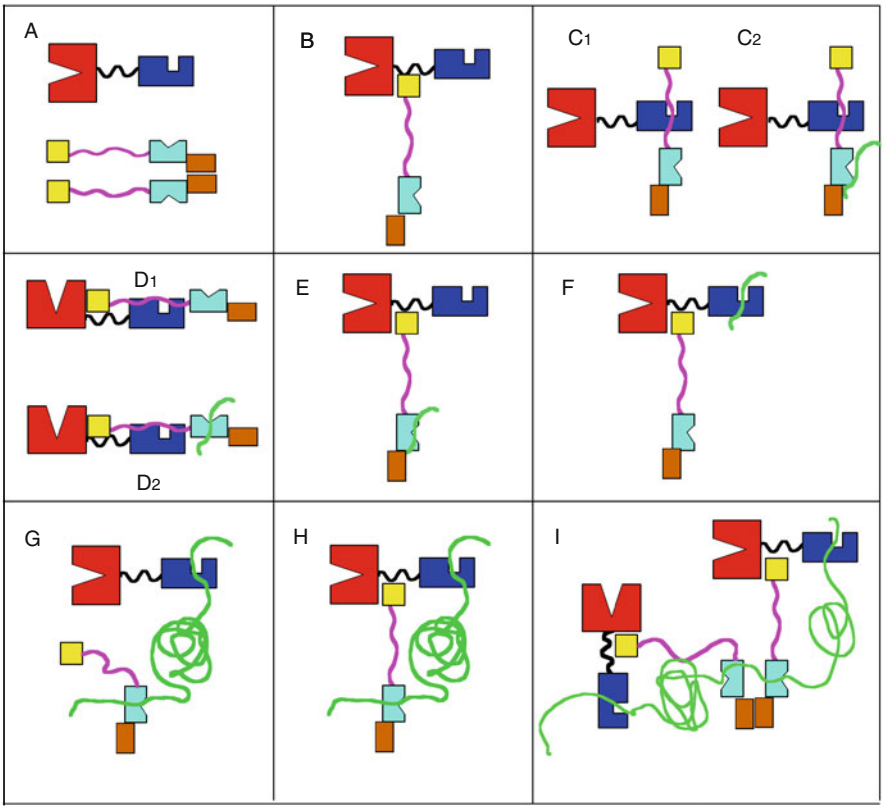

Fig. 18 Hypothetical binding modes between DnaK (*red*: NBD; *blue*: SBD), DnaJ (*yellow*: J-domain; *magenta*: G–F; *cyan*: SBD; *brown*: dimerization domain and substrate (*green*) in the ADP state

ATPase activity. At high concentrations, DnaJ itself serves as substrate for DnaK in a process considered to be unphysiological, where it stimulates ATP hydrolysis by DnaK > 1,000-fold [106].

A major and not yet resolved question in the field is whether DnaJ interacts more strongly with DnaK in the ADP or in the ATP state. Pierpaoli et al. [160] obtained a weak K_D value of >2 μM for the binding of DnaJ to DnaK.ATP and a strong K_D of 0.14 μM for the binding of DnaJ to a preformed 1:1 complex of DnaK and acrodylan-labeled CLLLSAPRR in the presence of ADP [160]. However, these results are contradicted by the following studies. Landry and co-workers have made a fusion of DnaJ (1–78) to CLLLSAPRR [153]. This J-fusion bound much more tightly to DnaK in the presence of ATP (0.2 nM) than in the absence of nucleotide (30 nM). A later paper of the same group using the same construct and using NMR spectroscopy to monitor binding to several DnaK constructs in different nucleotide states confirmed their earlier observations [161]. SPR experiments by Gross and co-workers [157] strongly suggest that wt-DnaJ binds tightly to the ATP state ($K_D = 70$ nM) but does not bind to DnaK in the ADP state (i.e., $K_D > 1$ μM).

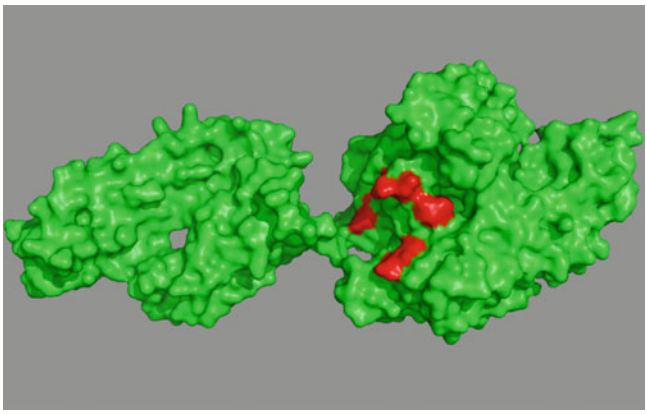

Fig. 19 The location of residues on *E. coli* DnaK that affect DnaK–DnaJ interaction as deduced from mutagenesis experiments (see text)

Single molecule fluorescence studies show that the yeast J protein Mdj1 is stably bound to yeast Hsp70 Ssc1 in the ATP state and dissociates upon ATP hydrolysis [96]. We have recently obtained results using NMR showing that DnaJ(1–70) binds at least ten times more tightly to DnaK(ATP-apo) than to the DnaK(ADP-sub). The majority of results thus suggest that DnaJ is poised to dissociate from DnaK once substrate is delivered.

While it is becoming clear how DnaJ interacts with DnaK, and how substrate and substrate-binding cleft are involved, it is much less clear which precise residues on the DnaK NBD interact with the J-domain. The DnaK mutations $YND_{145,147,148}AAA$ [86], $EV_{217,218}AA$ [86], and $R_{167}A$ [156] on the DnaK NBD domain weaken J–K interaction. All of these residues are found around the cleft area between subdomains IA and IIA of the NBD (see Fig. 19). However, mutations of these residues also affect the allosteric mechanism of DnaK itself, and it is unclear how the two effects intermingle. The mutant R167A is most interesting. Suh and co-workers [156] showed by SPR that the R167A mutant on DnaK could rescue the interaction of DnaJ D35N with DnaK. The effects were not dramatic (it "rescues" a K_D of 300 nM to a K_D of 100 nM). The R167H mutant had exactly the same rescuing capabilities as R167A. Potentially, Arg167 becomes buried in the complex with DnaJ. Such burial would be unfavorable if it is not compensated by buried negative charge in its vicinity. Hence, when the compensatory negative charge (D35) is mutated out, one must also mutate out burial of the positive charge to regain binding. The smallness of the effect argues for rather weak or remote D35 – R167 interaction. The SPR data strongly suggest that the J-domain interacts with NBD at a location that is now believed to be also the interaction site between the SBD and the NBD [38]. The interaction likely helps to establish or stabilize the DnaK state in which NBD and SBD do not interact.

A co-crystal structure of the NBD of Hsc70 with a J-domain of auxilin has been advanced [107]. The two proteins were covalently linked through disulfide chemistry between an Asp-Cys mutant at the equivalent location of Asp35 of DnaJ and an

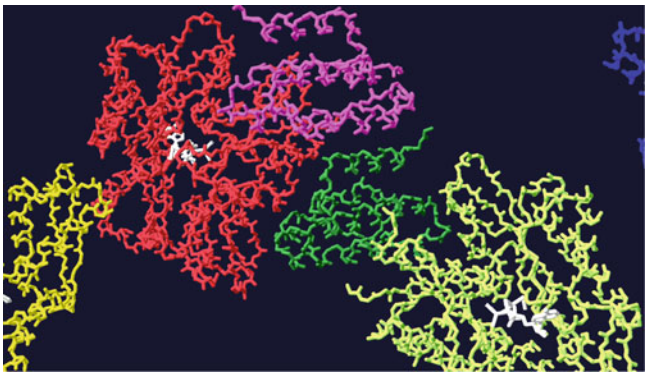

Fig. 20 Crystal contacts in the covalent adduct of human Auxilin (DnaJ homolog) and the NBD human Hsc70 [107]. The NBD and J-domain of the PDB-deposited adduct are in *light* and *dark green*, respectively. ADP is in *white*. The NBD and J-domain of the neighbor in the crystal are in *red* and *magenta*, respectively. The *green*" J-domain has a 372-Å^2 interface with its disulfide-linked Hsc70 NBD partner (*light green*). However, a symmetry-related NBD (*red*) has a 582 Å^2 interface with the same "*green*" J-domain (using www.ebi.ac.uk/msd-srv/prot_int/pistart.html). This figure was prepared using the Swiss PDB viewer

Arg-Cys mutant at the equivalent location of R167 in DnaK, as inspired by the work of Suh et al. [156]. This complex could potentially represent state E in Fig. 18. However, the complex is in the ADP state, and it is known from other work that the HPD loop is not involved in DnaJ–DnaK interaction in that state [152, 153]. In addition to questions about the validity of forcing the structure to a pre-determined pose by disulfide linking, the structure of this adduct is also rather suspect because crystal contacts between the J-domain of one "complex" with the NBD of another "complex" must affect the relative J-K orientations in the adduct (see Fig. 20).

Recently, using solution NMR, we obtained the three-dimensional conformation for a noncovalent Hsp70-DnaJ complex in the ADP state, loaded with substrate peptide [152]. The solution structure, which contained NBD, SBD, LID, substrate, and DnaJ(1–70), is completely different from the crystal structure of the adduct [107] (see Fig. 21). We establish that the J-domain (residues 1–70) binds with its positively charged helix II, which contains conserved residues that are critical to the interaction, as determined by mutagenesis [162], to a negatively charged area, ^{206}EIDEVDGEKTFEVLAT^{221} in the Hsp70 nucleotide-binding domain. In the crystal structure [107], this helix is not in the interface. The interface in the crystal (helix III) is not involved in contact in solution in the ADP state. The solution complex shows an unusual "tethered" binding mode which is stoichiometric and saturable, but which has a dynamic interface.

Recently, NMR data were published that suggest that DnaK residues 215–220 interact with the NBD-SBD linker in the ATP state but not in the ADP state [83]. It is significant that we [152] found that the J domain interacts with DnaK residues that contain this site, suggesting that its presence interferes with the docking of the linker, promoting the ADP conformation. This provides the long-awaited structural evidence for understanding how the J proteins regulate Hsp70 allostery.

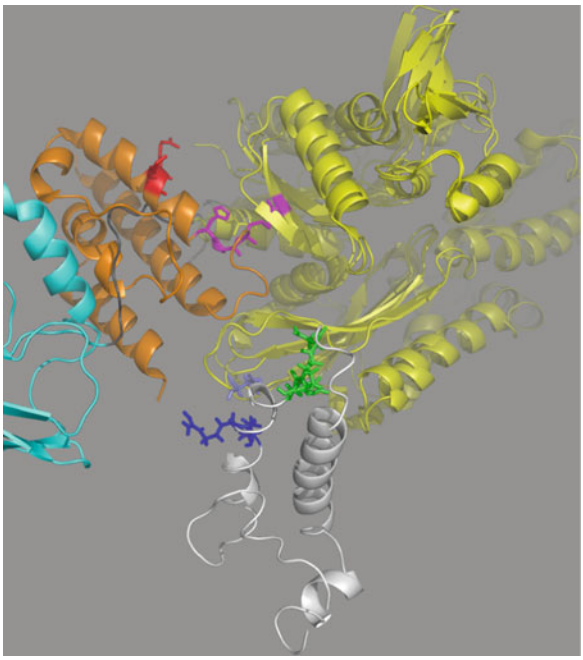

Fig. 21 The crystal structure [107] of the covalent adduct of Auxilin-J-domain (*orange*) and the NBD of human Hsc70 (*yellow*) superposed on the solution conformation [154] for the non-covalent complex of DnaJ-J-domain (*white*), DnaK NBD (*yellow*), NBD-SBD linker (*black*) and DnaK SBD (*cyan*). On Auxilin, the HPD loop and its covalent link to the NBD are in *purple* and the positive residues on helix II are *red*. On DnaJ, the HPD loop is *green*, and the positive residues on helix II are *blue*. Val210, in the center of the DnaK interface, is in *blue-gray*

13 Hsp70-Allosteric Effectors as Drugs

Consistent with its key role in protein homeostasis, Hsp70 chaperones have been implicated in numerous diseases. The various disease pathologies can be associated with "too much" Hsp70 activity (recycling of a toxic substrate) or with "too little" activity (failure to act on misfolded substrates). Thus, disease might arise from disruption of the delicately balanced proteostasis in either direction [163]. We will describe here just two disease classes, cancer and tauopathies, in which there is "too much" Hsp70 activity, so that one can conceivably aid in the therapy of these diseases by inhibiting Hsp70s.

All known tumors express elevated levels of Hsp70s [14]. One hypothesis is that the physiopathological features of the tumor microenvironment (low glucose, pH, and oxygen) mimic stress conditions [18, 19]. Alternatively, conformationally unstable oncoproteins may elicit a stress response [28, 164–167]. In cancer cells, Hsp70 stabilizes pro-survival factors [15–17] and inhibit cell death pathways [19, 22–26, 168, 169]. In addition, Hsp70 may prevent translocation of the apoptotic enhancer BAX from the cytosol to the mitochondria [170]. Hsp70 can also stabilize lysosomal membranes to inhibit the release of cathepsins and other enzymes which can induce cell death [171]. Hsp70 also plays roles in post-mitochondrial signaling pathways by antagonizing release of apoptogenic factors, such as cytochrome *c* and AIF [170]. Furthermore, Hsp70 can bind to and block the activity of APAF1 to avert the formation of the apoptosome and subsequent activation of caspase

enzymes [172]. Finally, Hsp70 also directly participates in oncogenic transformation [19]. One of the likely responsible mechanisms is the interaction of mitochondrial Hsp70 (mt-Hsp70) with mutant and wild-type tumor suppressor proteins, such as p53 [28, 166, 167, 173–175], and Rb107 [176]. The malignant transformation has been explained, in part, by the inactivation of p53 tumor suppressor protein by mt-Hsp70 [27]. In particular, wild-type p53 and mt-Hsp70 co-localize in the cytoplasm in several human cancers (undifferentiated neuroblastoma, retinoblastoma, colorectal and hepatocellular carcinomas, and glioblastoma) [28]. Together these observations support a model in which Hsp70 expression is anti-apoptotic and required for cancer cell viability. In addition, high expression of Hsp70 also confers resistance to chemotherapy, radiation, and hyperthermia therapy in breast cancer [18, 177]. Together, these observations suggest that Hsp70 is an important, potential drug target in cancer.

In support of these ideas, knockdown of Hsp70 chaperone expression [178, 179] or inhibition by small molecules [180] is lethal to cancer cell lines. For example, Hsp70 inhibitors generated by the Wipf and Brodsky groups have anti-proliferative activity against lung cancer cells [181] and Hsp70 inhibitors synthesized by the biotechnology company, Vernalis, have potent activity against cancer cells [182]. Moreover, a natural product, epigallocatechin gallate, interacts with Hsp70 [183] and triggers apoptosis in tumor cells [183]. MKT-077, a cationic rhodacyanine dye analog, which binds to Hsp70 [184], has activity against CX-1 colon carcinoma cells ($IC_{50} \sim 7\ \mu M$), but has no effect on normal epithelial cells [180]. Mechanistic studies indicated that MTK-077 inhibits the deleterious interaction of mt-Hsp70 with p53 by binding to the mt-Hsp70 NBD [167, 185]. These studies on MKT-077 generated significant excitement about this compound and it was advanced to phase I clinical trials [186]. However, MKT-077 was found to be nephrotoxic.

Many neurodegenerative disorders, such as Alzheimer's and Parkinson's diseases, are characterized by abnormal protein misfolding and accumulation [187–189]. In these disorders, misfolded proteins are not properly cleared by the chaperone/quality control system and, subsequently, they self-associate into cytotoxic oligomers. Diseases such as Alzheimer's are also characterized, besides beta plaques, by aberrant accumulation of hyperphosphorylated tau, called tau-tangles [29, 190–192]. Clearance of tau-tangles is being recognized as therapeutic to Alzheimer-affected neuronal cells [193]. Hsp70s participate in the clearance of tau-tangles through a mechanism that is in the process of being uncovered [194]. A key finding pertaining to this mechanism is that inhibitors of Hsp70 lead to a rapid increase in tau ubiquitination and proteasome-dependent degradation in tau-overexpressing HeLa cells [195]. Conversely, activators of Hsp70 led to a decrease proteasome-dependent degradation of tau. Thus, it seems that inhibition of Hsp70 is a potential target for helping the clearance of tau and a first step towards a therapy of CNS disorders.

As evident throughout this review, Hsp70s are highly allosteric enzymes that engage in a number of critical protein–protein interactions. Thus, Hsp70s proteins must be very druggable [196] because they offer so many opportunities for interference (Fig. 22). The most obvious sites for designing inhibitors are the primary

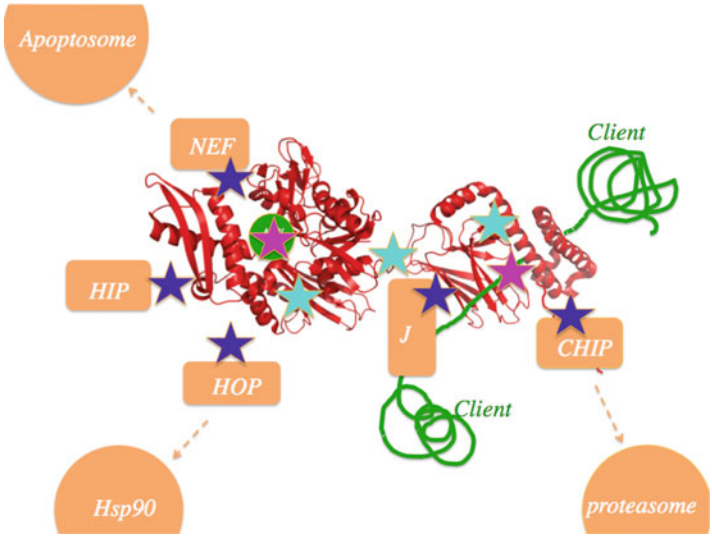

Fig. 22 Potential sites for interference with the Hsp70 chaperone function. *Purple*: primary sites, *cyan*: allosteric sites, *blue*: co-chaperone interaction sites

ATP and substrate-binding pockets. Such deep clefts are often associated with favorable progress in drug discovery campaigns. In fact, both of these binding sites have been explored [197, 198] and some of the resulting compounds have promising anti-cancer and anti-bacterial activity. However, these pockets have a number of features that make them challenging. For example, the nucleotide-binding cassette of Hsp70s is highly conserved, creating problems in selectivity. Similarly, the substrate-binding cleft of the Hsp70s is designed to be promiscuous and capable of binding many hydrophobic sequences; thus, it is expected to be difficult to generate soluble, selective compounds for that region. Another potential problem with these strategies is that they would be expected to "lock" Hsp70s into a specific structure in the ensemble. Namely, competitive ATP-competitive inhibitors might lock the protein into the ATP-bound form, while substrate-based inhibitors would favor the substrate-bound form. As discussed in this review, there are many other states of Hsp70 and these might also be linked to aspects of disease. Thus, one can also imagine directing Hsp70 function in new ways by targeting its interactions with DnaJ co-chaperones or nucleotide exchange factors [3]. Hsp70s also interact with HIP [199], HOP [200], and CHIP [201], and some specialized factors such as ZIM (for mt-Hsp70) [202]. In theory, competing with these contacts or even enhancing their recruitment may be another, parallel avenue for modulating the activity and structure of Hsp70s. The potential advantage of this approach is that the activity of the Hsp70 complex might be "tuned" to achieve the desired outcomes.

In theory, compounds with activities at allosteric and protein–protein sites might either directly interfere with co-chaperone interactions or they might recognize allosteric differences and perturb the allosteric equilibrium between states of

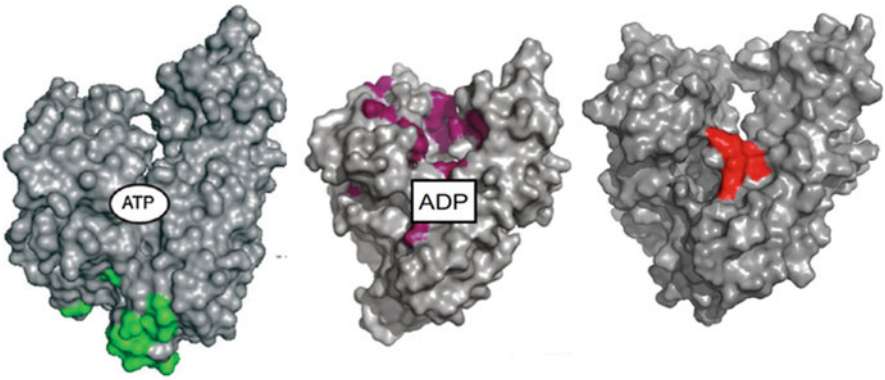

Fig. 23 The NMR-determined binding sites of recently discovered Hsp70 inhibitors. *Left*, 115-7C [203]; *middle*, myricetin [204]; *right*, MKT-077 [205]. Note that neither compound binds to an Hsp70 primary site, hence the compounds affect Hsp70 function by affecting allostery or co-chaperone interaction

Hsp70. Consistent with this idea, we recently discovered one class of DnaK inhibitors that functions by directly competing with the J protein interaction [203] (see Fig. 23a) and another class of compounds, including the flavonoid myricetin, which bind to a site on DnaK that is >30 Å from the DnaJ binding site to block this interaction allosterically [204] (Fig. 23b). These studies suggest that Hsp70s, such as DnaK, do indeed have multiple opportunities for pharmacologic intervention, including at sites that might not be anticipated from cursory examination of the structures.

Many of the emerging methods for targeting Hsp70 are likely to take advantage of the allostery in this target. For example, compounds that can recognize allosteric differences and perturb the allosteric equilibrium between the states should also modulate Hsp70s function. To illustrate this idea, we recently discovered that the anti-cancer compound MKT-077 is an allosteric inhibitor of Hsp70. MKT-077 [184, 206] was originally considered as a potential therapy for the treatment of breast cancer [207]. Later it was suggested that MKT-077 kills cancer cells by selectively inhibiting mt-Hsp70 [187]. However, the mechanism of MKT-077 wasn't clear and its potential binding site of Hsp70s was unknown. Based on the high homology between mt-Hsp70 and other Hsp70s, we reasoned that MKT-077 may also bind to cytosolic homologs, such as Hsc70 and Hsp70. Consistent with this idea, MKT-077 binds with an affinity of approximately 10 μM to human Hsc70 NBD (determined by NMR [205]). This value is remarkably close to the $IC_{50} \sim 7$ μM for MKT-077 activity against CX-1 colon carcinoma cells [180]. Also consistent with its cytosolic actions, MKT-077 clears tau in a dose-dependent manner in HeLa cells [205]. This activity may be therapeutically important because other compounds that reduce tau accumulation through Hsp70s recover cognitive function in mouse models of Alzheimer's disease [208].

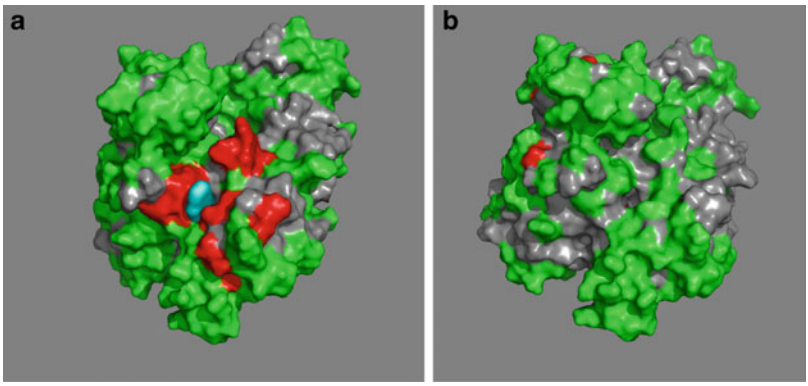

Fig. 24 (**a**) Chemical shifts seen [205] for the interaction of MKT-077 (*cyan*) with human Hsc70 in the ADP state. (**b**) Chemical shifts seen [205] for the interaction of MKT-077 with human Hsc70 in the AMP-PNP state

To help development of more potent MKT-077 derivatives, we investigated where the compound binds to Hsc70 [205]. The first finding was that MKT-077 binds to the Hsc70 ADP state, but that no binding to the ATP state could be detected (i.e., $K_D > 100$ μM) (Fig. 24). Thus, we hypothesized that MKT-077 might trap Hsp70 in the ADP-bound, high-affinity form. This hypothesis was supported by partial proteolysis findings, which suggested that MKT-077 stabilizes the ADP-bound conformation of full length Hsp70s. Although the mechanisms linking this allosteric switch to the degradation of tau is not yet clear, it seems possible that the long-lived Hsp70-ADP-tau complex becomes a good target for CHIP, an E3 ubiquitin ligase that binds Hsp70s. If so, then this "stalled" complex would favor the polyubiquitination and degradation of Hsp70-bound tau [201, 209].

How does MKT-077 distinguish between the NBD ADP and ATP state? It turns out that MKT-077 binds to a pocket that is close, but not identical, to the nucleotide-binding site (see Fig. 24). According to our earlier studies of the NBD of DnaK *T. Thermophilus*, ADP and AMPPNP cause significant changes in NBD subunit orientations [82], which affects the area where the MKT-077 pocket is located. However, in that study we did not carry out a high resolution structure determination. Rather, we suggested that the nucleotide-induced changes were not unlike those seen between crystal structures of Hsp70 in nucleotide-bound form (a representative of the ATP state) and those of Hsc70 bound to nucleotide exchange factors, (more representative of the ADP state). In Fig. 25 we show the difference between these crystal structures. Indeed, only in the ADP state is there a pocket available that can accommodate MKT-077. The pocket is smaller in the ATP state. Therefore, MKT-077 is an allosteric effector, and acts not unlike 2,3-DPG which down-regulates hemoglobin oxygen affinity by binding to a non-heme site that is open in the T-state and closed in the R-state [210]

Subsequently, we modeled the binding of MKT-077 on the conformation of Hsc70 NBD as seen in a complex containing NEF. The NMR chemical shift

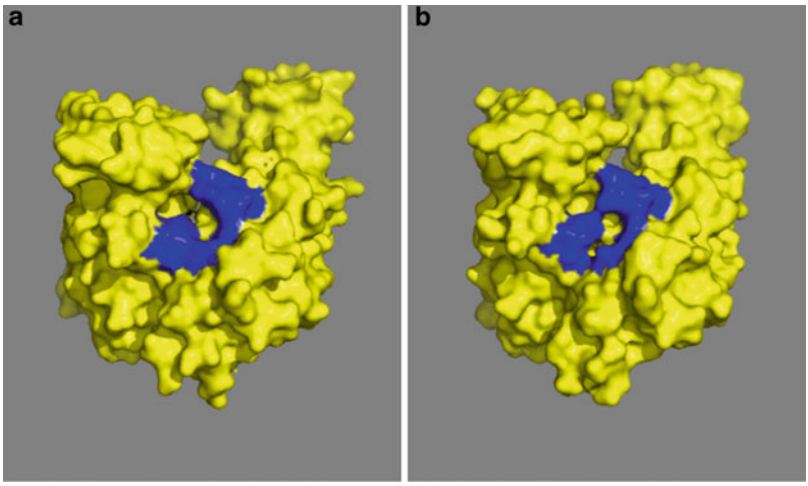

Fig. 25 (**a**) The MKT-077 binding site [205] (*blue*) projected on human Hsc70 NBD in the open state (complexed with NEF; 3C7N.pdb) (**b**). The MKT-077 binding site (*blue*) projected on Hsc70 NBD in the closed state (3HSC.pdb)

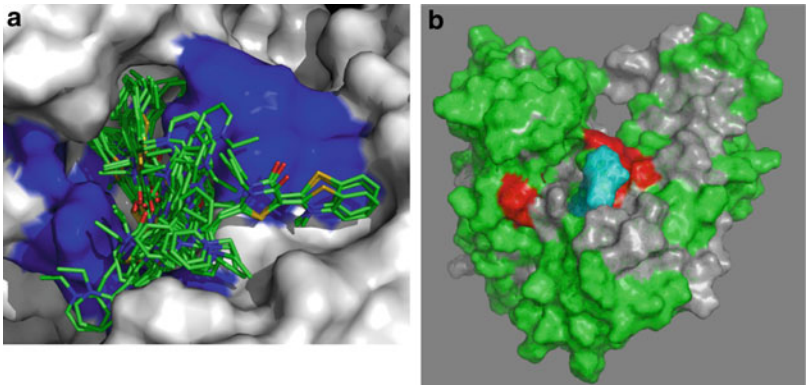

Fig. 26 The MKT-077 Hsc70 NBD interaction in detail [205]. (**a**) Collection of poses for the binding of MKT077 to Hsc70 (3C7N.pdb) obtained from NMR restrained AUTODOCK. *Blue*: NMR shifts. (**b**) Final best binding pose of MKT077 (*cyan*) on Hsc70 (3C7N.pdb) obtained with AMBER. *Green*: no shifts; *red*: shifts; *gray*: undecided

perturbations were used to constrain the search box in the AUTODOCK [211] docking program. AUTODOCK produced four families of binding poses that were energetically equivalent, but which differed as much as having different rings of MKT-077 inside or outside the pocket (Fig. 26a). We decided to carry out AMBER molecular dynamics [212] simulated annealing computations using Hsc70 in explicit water, starting with representatives of the four different AUTODOCK families. After equilibrium was reached, we evaluated the AMBER binding energy using the MM-GB/PBSA protocol [213]. As a result, one particular family of poses

stood out. This pose is shown in Fig. 26b. It forms the basis for our further drug development endeavors.

Together, these results, while quite preliminary, suggest that Hsp70s may be targets for cancer and CNS disorders through a variety of direct and allosteric mechanisms. Hopefully, a larger battery of Hsp70 inhibitors with defined mechanisms-of-action will become available and these reagents will, in turn, allow new insights into the roles of Hsp70s in disease.

14 Outlook

The Hsp70/DnaJ/NEF system is complicated and subtle. Different scientific disciplines uncover seemingly unrelated and sometimes contradictory facts about the system. Clearly, much more research is required to uncover all aspects of the Hsp70/DnaJ/NEF system. In addition, the Hsp70s interact with many co-factors such as HIP, HOP, and CHIP. In most cases not even structures of such complexes are known, let alone the subtleties of the energetics and dynamics of these interactions. We hope that support for many more years of Hsp70 research will be forthcoming. It should be well worth it, given the fact that disregulation of Hsp70s is involved in diseases that affect much of humanity.

Acknowledgements Support from NIH grants GM63027-S02 (ERPZ, AA), NS059690 (AR, ERPZ and JEG) is gratefully acknowledged. An anonymous reviewer is gratefully acknowledged for suggesting many improvements to the manuscript.

References

1. Hightower LE (1991) Heat-shock, stress proteins, chaperones, and proteotoxicity. Cell 66:191–197
2. Marques C, Guo W, Pereira P, Taylor A, Patterson C, Evans PC, Shang F (2006) The triage of damaged proteins: degradation by the ubiquitin-proteasome pathway or repair by molecular chaperones. FASEB J 20:741–743
3. Bukau B, Weissman J, Horwich A (2006) Molecular chaperones and protein quality control. Cell 125:443–451
4. Sfatos CD, Gutin AM, Abkevich VI, Shakhnovich EI (1996) Simulations of chaperone-assisted folding. Biochemistry 35:334–339
5. Gupta RS (1998) Protein phylogenies and signature sequences: a reappraisal of evolutionary relationships among archaebacteria, eubacteria, and eukaryotes. Microbiol Mol Biol Rev 62:1435–1491
6. Zylicz M, Wawrzynow A (2001) Insights into the function of Hsp70 chaperones. IUBMB Life 51:283–287
7. Qian S-B, McDonough H, Boellmann F, Cyr DM, Patterson C (2006) CHIP-mediated stress recovery by sequential ubiquitination of substrates and Hsp70. Nature 440:551–555
8. Majeski AE, Dice JF (2004) Mechanisms of chaperone-mediated autophagy. Int J Biochem Cell Biol 36:2435–2444

9. Craig EA, Huang P, Aron R, Andrew A (2006) The diverse roles of J-proteins, the obligate Hsp70 co-chaperone. Rev Physiol Biochem Pharmacol 156:1–21
10. Tzankov S, Wong MJ, Shi K, Nassif C, Young JC (2008) Functional divergence between co-chaperones of Hsc70. J Biol Chem 283:27100–27109
11. Chappell TG, Konforti BB, Schmid SL, Rothman JE (1987) The ATPase core of a clathrin uncoating protein. J Biol Chem 262:746–751
12. Brinker A, Scheufler C, Von Der Mulbe F, Fleckenstein B, Herrmann C, Jung G, Moarefi I, Hartl FU (2002) Ligand discrimination by TPR domains. Relevance and selectivity of EEVD-recognition in Hsp70 x Hop x Hsp90 complexes. J Biol Chem 277:19265–19275
13. Wells AD, Rai SK, Salvato MS, Band H, Malkovsky M (1997) Restoration of MHC class I surface expression and endogenous antigen presentation by a molecular chaperone. Scand J Immunol 45:605–612
14. Shin BK, Wang H, Yim AM, Le Naour F, Brichory F, Jang JH, Zhao R, Puravs E, Tra J, Michael CW, Misek DE, Hanash SM (2003) Global profiling of the cell surface proteome of cancer cells uncovers an abundance of proteins with chaperone function. J Biol Chem 278:7607–7616
15. Nylandsted J, Brand K, Jaattela M (2000) Heat shock protein 70 is required for the survival of cancer cells. Ann N Y Acad Sci 926:122–125
16. Kaul Z, Yaguchi T, Kaul SC, Hirano T, Wadhwa R, Taira K (2003) Mortalin imaging in normal and cancer cells with quantum dot immuno-conjugates. Cell Res 13:503–507
17. Kaul SC, Yaguchi T, Taira K, Reddel RR, Wadhwa R (2003) Overexpressed mortalin (mot-2)/mthsp70/GRP75 and hTERT cooperate to extend the in vitro lifespan of human fibroblasts. Exp Cell Res 286:96–101
18. Ciocca DR, Calderwood SK (2005) Heat shock proteins in cancer: diagnostic, prognostic, predictive, and treatment implications. Cell Stress Chaperones 10:86–103
19. Garrido C, Brunet M, Didelot C, Zermati Y, Schmitt E, Kroemer G (2006) Heat shock proteins 27 and 70: anti-apoptotic proteins with tumorigenic properties. Cell Cycle 5:2592–2601
20. Soti C, Csermely P (2002) Chaperones and aging: role in neurodegeneration and in other civilizational diseases. Neurochem Int 41:383–389
21. Soti C, Csermely P (2002) Chaperones come of age. Cell Stress Chaperones 7:186–190
22. Abarzua F, Sakaguchi M, Tanimoto R, Sonegawa H, Li DW, Edamura K, Kobayashi T, Watanabe M, Kashiwakura Y, Kaku H, Saika T, Nakamura K, Nasu Y, Kumon H, Huh NH (2007) Heat shock proteins play a crucial role in tumor-specific apoptosis by REIC/Dkk-3. Int J Mol Med 20:37–43
23. Lanneau D, Brunet M, Frisan E, Solary E, Fontenay M, Garrido C (2008) Heat shock proteins: essential proteins for apoptosis regulation. J Cell Mol Med 12:743–761
24. Calderwood SK, Ciocca DR (2008) Heat shock proteins: stress proteins with Janus-like properties in cancer. Int J Hyperthermia 24:31–39
25. Beere HM, Wolf BB, Cain K, Mosser DD, Mahboubi A, Kuwana T, Tailor P, Morimoto RI, Cohen GM, Green DR (2000) Heat-shock protein 70 inhibits apoptosis by preventing recruitment of procaspase-9 to the Apaf-1 apoptosome. Nat Cell Biol 2:469–475
26. Garrido C, Schmitt E, Cande C, Vahsen N, Parcellier A, Kroemer G (2003) Hsp27 and Hsp70: potentially oncogenic apoptosis inhibitors. Cell Cycle 2:579–584
27. Kaul SC, Duncan EL, Englezou A, Takano S, Reddel RR, Mitsui Y, Wadhwa R (1998) Malignant transformation of NIH3T3 cells by overexpression of mot-2 protein. Oncogene 17:907–911
28. Walker C, Bottger S, Low B (2006) Mortalin-based cytoplasmic sequestration of p53 in a nonmammalian cancer model. Am J Pathol 168:1526–1530
29. Buee L, Bussiere T, Buee-Scherrer V, Delacourte A, Hof PR (2000) Tau protein isoforms, phosphorylation and role in neurodegenerative disorders. Brain Res Rev 33:95–130
30. Flaherty KM, Deluca-Flaherty C, McKay DB (1990) 3-Dimensional structure of the ATPase fragment of a 70 k heat-shock cognate protein. Nature 346:623–628

31. Bork P, Sander C, Valencia A (1992) An ATPase domain common to prokaryotic cell-cycle proteins, sugar kinases, actin, and Hsp70 heat-shock proteins. Proc Natl Acad Sci USA 89:7290–7294
32. O'Brien MC, Flaherty KM, McKay DB (1996) Lysine 71 of the chaperone protein Hsc70 Is essential for ATP hydrolysis. J Biol Chem 271:15874–15878
33. Wilbanks SM, DeLuca-Flaherty C, McKay DB (1994) Structural basis of the 70-kilodalton heat shock cognate protein ATP hydrolytic activity. I. Kinetic analyses of active site mutants. J Biol Chem 269:12893–12898
34. O'Brien MC, McKay DB (1995) How potassium affects the activity of the molecular chaperone Hsc70.I. Potassium is required for optimal ATPase activity. J Biol Chem 270:2247–2250
35. Vogel M, Mayer MP, Bukau B (2006) Allosteric regulation of Hsp70 chaperones involves a conserved interdomain linker. J Biol Chem 281:38705–38711
36. Morshauser RC, Wang H, Flynn GC, Zuiderweg ER (1995) The peptide-binding domain of the chaperone protein Hsc70 has an unusual secondary structure topology. Biochemistry 34:6261–6266
37. Zhu XT, Zhao X, Burkholder WF, Gragerov A, Ogata CM, Gottesman ME, Hendrickson WA (1996) Structural analysis of substrate binding by the molecular chaperone DnaK. Science 272:1606–1614
38. Bertelsen EB, Chang L, Gestwicki JE, Zuiderweg ERP (2009) Solution conformation of wild-type E. coli Hsp70 (DnaK) chaperone complexed with ADP and substrate. Proc Natl Acad Sci USA 106:8471–8476
39. Smock RG, Blackburn ME, Gierasch LM (2011) Conserved, disordered C terminus of DnaK enhances cellular survival upon stress and DnaK in vitro chaperone activity. J Biol Chem 286:31821–31829
40. Pidoux AL, Armstrong J (1992) Analysis of the BIP gene and identification of an ER retention signal in S. Pombe. EMBO J 11:1583–1591
41. Bukau B, Horwich AL (1998) The Hsp70 and Hsp60 chaperone machines. Cell 92:351–366
42. Han WJ, Christen P (2003) Mechanism of the targeting action of DnaJ in the DnaK molecular chaperone system. J Biol Chem 278:19038–19043
43. Moreno-del Alamo M, Sanchez-Gorostiaga A, Serrano AM, Prieto A, Cuellar J, Martin-Benito J, Valpuesta JM, Giraldo R (2010) Structural analysis of the interactions between Hsp70 chaperones and the yeast DNA replication protein Orc4p. J Mol Biol 403:24–39
44. Mayer MP, Bukau B (2005) Hsp70 chaperones: cellular functions and molecular mechanism. Cell Mol Life Sci 62:670–684
45. Schroder H, Langer T, Hartl FU, Bukau B (1993) Dnak Dnaj and Grpe form a cellular chaperone machinery capable of repairing heat-induced protein damage. EMBO J 12:4137–4144
46. Ziemienowicz A, Skowyra D, Zeilstra-Ryalls J, Fayet O, Georgopoulos C, Zylicz M (1993) Both the Escherichia coli chaperone systems, GroEL/GroES and DnaK/DnaJ/GrpE, can reactivate heat-treated RNA polymerase. Different mechanisms for the same activity. J Biol Chem 268:25425–25431
47. Diamant S, Ben-Zvi AP, Bukau B, Goloubinoff P (2000) Size-dependent disaggregation of stable protein aggregates by the DnaK chaperone machinery. J Biol Chem 275:21107–21113
48. Hartl FU, Hayer-Hartl M (2002) Molecular chaperones in the cytosol: from nascent chain to folded protein. Science 295:1852–1858
49. Yam AY, Xia Y, Lin HTJ, Burlingame A, Gerstein M, Frydman J (2008) Defining the TRiC/CCT interactome links chaperonin function to stabilization of newly made proteins with complex topologies. Nat Struct Mol Biol 15:1255–1262
50. De los Rios P, Ben-Zvi A, Slutsky O, Azem A, Goloubinoff P (2006) Hsp70 chaperones accelerate protein translocation and the unfolding of stable protein aggregates by entropic pulling. Proc Natl Acad Sci USA 103:6166–6171
51. Sharma SK, De Los Rios P, Christen P, Lustig A, Goloubinoff P (2010) The kinetic parameters and energy cost of the Hsp70 chaperone as a polypeptide unfoldase. Nat Chem Biol 6:914–920

52. Goloubinoff P, De Los Rios P (2007) The mechanism of Hsp70 chaperones: (entropic) pulling the models together. Trends Biochem Sci 32:372–380
53. Szabo A, Langer T, Schroder H, Flanagan J, Bukau B, Hartl FU (1994) The ATP hydrolysis-dependent reaction cycle of the Escherichia coli Hsp70 system DnaK, DnaJ, and GrpE. Proc Natl Acad Sci USA 91:10345–10349
54. Mayer MP, Rudiger S, Bukau B (2000) Molecular basis for interactions of the DnaK chaperone with substrates. Biol Chem 381:877–885
55. Schmid D, Baici A, Gehring H, Christen P (1994) Kinetics of molecular chaperone action. Science 263:971–973
56. McCarty JS, Buchberger A, Reinstein J, Bukau B (1995) The role of ATP in the functional cycle of the DnaK chaperone system. J Mol Biol 249:126–137
57. Kim DH, Lee YJ, Corry PM (1992) Constitutive Hsp70-oligomerization and its dependence on ATP binding. J Cell Physiol 153:353–361
58. Chang L, Bertelsen EB, Wisen S, Larsen EM, Zuiderweg ERP, Gestwicki JE (2008) High-throughput screen for small molecules that modulate the ATPase activity of the molecular chaperone DnaK. Anal Biochem 372:167–176
59. Jayakumar J, Smolenski RT, Gray CC, Goodwin AT, Kalsi K, Amrani M, Yacoub MH (1998) Influence of heat stress on myocardial metabolism and functional recovery after cardioplegic arrest: a P-31 NMR study. Eur J Cardiothorac Surg 13:467–474
60. Theyssen H, Schuster HP, Packschies L, Bukau B, Reinstein J (1996) The second step of ATP binding to DnaK induces peptide release. J Mol Biol 263:657–670
61. Buchberger A, Theyssen H, Schroder H, McCarty JS, Virgallita G, Milkereit P, Reinstein J, Bukau B (1995) Nucleotide-induced conformational changes in the ATPase and substrate binding domains of the DnaK chaperone provide evidence for interdomain communication. J Biol Chem 270:16903–16910
62. Montgomery DL, Morimoto RI, Gierasch LM (1999) Mutations in the substrate binding domain of the Escherichia coli 70 kDa molecular chaperone, DnaK, which alter substrate affinity or interdomain coupling. J Mol Biol 286:915–932
63. Rist W, Graf C, Bukau B, Mayer MP (2006) Amide hydrogen exchange reveals conformational changes in hsp70 chaperones important for allosteric regulation. J Biol Chem 281:16493–16501
64. Revington M, Zhang Y, Yip GN, Kurochkin AV, Zuiderweg ER (2005) NMR investigations of allosteric processes in a two-domain Thermus thermophilus Hsp70 molecular chaperone. J Mol Biol 349:163–183
65. Swain JF, Dinler G, Sivendran R, Montgomery DL, Stotz M, Gierasch LM (2007) Hsp70 chaperone ligands control domain association via an allosteric mechanism mediated by the interdomain linker. Mol Cell 26:27–39
66. Bukau B, Walker GC (1989) Cellular defects caused by deletion of the Escherichia coli dnaK gene indicate roles for heat shock protein in normal metabolism. J Bacteriol 171:2337–2346
67. Georgopoulos CP (1977) New bacterial gene (Gropc) which affects lambda-DNA replication. Mol Gen Genet 151:35–39
68. Schlecht R, Erbse AH, Bukau B, Mayer MP (2011) Mechanics of Hsp70 chaperones enables differential interaction with client proteins. Nat Struct Mol Biol 18:345–351
69. Chang L, Thompson AD, Ung P, Carlson HA, Gestwicki JE (2010) Mutagenesis reveals the complex relationships between ATPase rate and the chaperone activities of Escherichia coli heat shock protein 70 (Hsp70/DnaK). J Biol Chem 285:21282–21291
70. Flaherty KM, Wilbanks SM, DeLuca-Flaherty C, McKay DB (1994) Structural basis of the 70-kilodalton heat shock cognate protein ATP hydrolytic activity. II. Structure of the active site with ADP or ATP bound to wild type and mutant ATPase fragment. J Biol Chem 269:12899–12907
71. Harrison CJ, Hayer-Hartl M, Di Liberto M, Hartl F, Kuriyan J (1997) Crystal structure of the nucleotide exchange factor GrpE bound to the ATPase domain of the molecular chaperone DnaK. Science 276:431–435

72. Osipiuk J, Walsh MA, Freeman BC, Morimoto RI, Joachimiak A (1999) Structure of a new crystal form of human Hsp70 ATPase domain. Acta Crystallogr D Biol Crystallogr 55:1105–1107
73. Morshauser RC, Hu W, Wang H, Pang Y, Flynn GC, Zuiderweg ER (1999) High-resolution solution structure of the 18 kDa substrate-binding domain of the mammalian chaperone protein Hsc70. J Mol Biol 289:1387–1403
74. Pellecchia M, Montgomery DL, Stevens SY, Vander Kooi CW, Feng HP, Gierasch LM, Zuiderweg ER (2000) Structural insights into substrate binding by the molecular chaperone DnaK. Nat Struct Biol 7:298–303
75. Bertelsen EB, Zhou H, Lowry DF, Flynn GC, Dahlquist FW (1999) Topology and dynamics of the 10 kDa C-terminal domain of DnaK in solution. Protein Sci 8:343–354
76. Jiang J, Prasad K, Lafer EM, Sousa R (2005) Structural basis of interdomain communication in the Hsc70 chaperone. Mol Cell 20:513–524
77. Chang YW, Sun YJ, Wang C, Hsiao CD (2008) Crystal structures of the 70-kDa heat shock proteins in domain disjoining conformation. J Biol Chem 283:15502–15511
78. Wang H, Pang Y, Kurochkin AV, Hu W, Flynn GC, Zuiderweg ERP (1998) The solution structure of the 21 kDa chaperone protein DnaK substrate binding domain: a preview of chaperone - protein interaction. Biochemistry 37:7929–7940
79. Swain JF, Schulz EG, Gierasch LM (2006) Direct comparison of a stable isolated Hsp70 substrate-binding domain in the empty and substrate-bound states. J Biol Chem 281:1605–1611
80. Liu Q, Hendrickson WA (2007) Insights into hsp70 chaperone activity from a crystal structure of the yeast Hsp110 Sse1. Cell 131:106–120
81. Zhang Y, Zuiderweg ER (2004) The 70-kDa heat shock protein chaperone nucleotide-binding domain in solution unveiled as a molecular machine that can reorient its functional subdomains. Proc Natl Acad Sci USA 101:10272–10277
82. Bhattacharya A, Kurochkin AV, Yip GN, Zhang Y, Bertelsen EB, Zuiderweg ER (2009) Allostery in Hsp70 chaperones is transduced by subdomain rotations. J Mol Biol 388:475–490
83. Zhuravleva A, Gierasch LM (2011) Allosteric signal transmission in the nucleotide-binding domain of 70-kDa heat shock protein (Hsp70) molecular chaperones. Proc Natl Acad Sci USA 108:6987–6992
84. Sousa MC, McKay DB (1998) The hydroxyl of threonine 13 of the bovine 70-kDa heat shock cognate protein is essential for transducing the ATP-induced conformational change. Biochemistry 37:15392–15399
85. O'Brien MC, McKay DB (1993) Threonine 204 of the chaperone protein Hsc70 influences the structure of the active site, but is not essential for ATP hydrolysis. J Biol Chem 268:24323–24329
86. Gassler CS, Buchberger A, Laufen T, Mayer MP, Schroder H, Valencia A, Bukau B (1998) Mutations in the DnaK chaperone affecting interaction with the DnaJ cochaperone. Proc Natl Acad Sci USA 95:15229–15234
87. Barthel TK, Zhang J, Walker GC (2001) ATPase-defective derivatives of Escherichia coli DnaK that behave differently with respect to ATP-induced conformational change and peptide release. J Bacteriol 183:5482–5490
88. Rudiger S, Mayer MP, Schneider-Mergener J, Bukau B (2000) Modulation of substrate specificity of the DnaK chaperone by alteration of a hydrophobic arch. J Mol Biol 304:245–251
89. Vogel M, Bukau B, Mayer MP (2006) Allosteric regulation of Hsp70 chaperones by a proline switch. Mol Cell 21:359–367
90. Han W, Christen P (2001) Mutations in the interdomain linker region of DnaK abolish the chaperone action of the DnaK/DnaJ/GrpE system. FEBS Lett 497:55–58
91. Burkholder WF, Zhao X, Zhu X, Hendrickson WA, Gragerov A, Gottesman ME (1996) Mutations in the C-terminal fragment of DnaK affecting peptide binding. Proc Natl Acad Sci USA 93:10632–10637

92. Voisine C, Craig EA, Zufall N, von Ahsen O, Pfanner N, Voos W (1999) The protein import motor of mitochondria: unfolding and trapping of preproteins are distinct and separable functions of matrix Hsp70. Cell 97:565–574
93. Smock RG, Rivoire O, Russ WP, Swain JF, Leibler S, Ranganathan R, Gierasch LM (2010) An interdomain sector mediating allostery in Hsp70 molecular chaperones. Mol Syst Biol 6:414
94. Shi L, Kataoka M, Fink AL (1996) Conformational characterization of DnaK and its complexes by small-angle X-ray scattering. Biochemistry 35:3297–3308
95. Wilbanks SM, Chen L, Tsuruta H, Hodgson KO, McKay DB (1995) Solution small-angle X-ray scattering study of the molecular chaperone Hsc70 and its subfragments. Biochemistry 34:12095–12106
96. Mapa K, Sikor M, Kudryavtsev V, Waegemann K, Kalinin S, Seidel CAM, Neupert W, Lamb DC, Mokranjac D (2010) The conformational dynamics of the mitochondrial Hsp70 chaperone. Mol Cell 38:89–100
97. Buczynski G, Slepenkov SV, Sehorn MG, Witt SN (2001) Characterization of a lidless form of the molecular chaperone DnaK: deletion of the lid increases peptide on- and off-rate constants. J Biol Chem 276:27231–27236
98. Slepenkov SV, Witt SN (2002) Kinetic analysis of interdomain coupling in a lidless variant of the molecular chaperone DnaK: DnaK's lid inhibits transition to the low affinity state. Biochemistry 41:12224–12235
99. Chesnokova LS, Slepenkov SV, Protasevich II, Sehorn MG, Brouillette CG, Witt SN (2003) Deletion of DnaK's lid strengthens binding to the nucleotide exchange factor, GrpE: a kinetic and thermodynamic analysis. Biochemistry 42:9028–9040
100. Slepenkov SV, Patchen B, Peterson KM, Witt SN (2003) Importance of the D and E helices of the molecular chaperone DnaK for ATP binding and substrate release. Biochemistry 42:5867–5876
101. Slepenkov SV, Witt SN (1998) Kinetics of the reactions of the Escherichia coli molecular chaperone DnaK with ATP: evidence that a three-step reaction precedes ATP hydrolysis. Biochemistry 37:1015–1024
102. Slepenkov SV, Witt SN (1998) Peptide-induced conformational changes in the molecular chaperone DnaK. Biochemistry 37:16749–16756
103. Slepenkov SV, Witt SN (2002) The unfolding story of the Escherichia coli Hsp70 DnaK: is DnaK a holdase or an unfoldase? Mol Microbiol 45:1197–1206
104. Slepenkov SV, Witt SN (2003) Detection of a concerted conformational change in the ATPase domain of DnaK triggered by peptide binding. FEBS Lett 539:100–104
105. Buchberger A, Valencia A, McMacken R, Sander C, Bukau B (1994) The chaperone function of DnaK requires the coupling of ATPase activity with substrate binding through residue E171. Embo J 13:1687–1695
106. Laufen T, Mayer MP, Beisel C, Klostermeier D, Mogk A, Reinstein J, Bukau B (1999) Mechanism of regulation of hsp70 chaperones by DnaJ cochaperones. Proc Natl Acad Sci USA 96:5452–5457
107. Jiang J, Maes EG, Taylor AB, Wang L, Hinck AP, Lafer EM, Sousa R (2007) Structural basis of J cochaperone binding and regulation of Hsp70. Mol Cell 28:422–433
108. Revington M, Holder TM, Zuiderweg ER (2004) NMR study of nucleotide-induced changes in the nucleotide binding domain of Thermus thermophilus Hsp70 chaperone DnaK: implications for the allosteric mechanism. J Biol Chem 279:33958–33967
109. Fischer MW, Losonczi JA, Weaver JL, Prestegard JH (1999) Domain orientation and dynamics in multidomain proteins from residual dipolar couplings. Biochemistry 38:9013–9022
110. Sondermann H, Scheufler C, Schneider C, Hohfeld J, Hartl FU, Moarefi I (2001) Structure of a Bag/Hsc70 complex: convergent functional evolution of Hsp70 nucleotide exchange factors. Science 291:1553–1557

111. Shomura Y, Dragovic Z, Chang HC, Tzvetkov N, Young JC, Brodsky JL, Guerriero V, Hartl FU, Bracher A (2005) Regulation of Hsp70 function by HspBP1: structural analysis reveals an alternate mechanism for Hsp70 nucleotide exchange. Mol Cell 17:367–379
112. Dragovic Z, Broadley SA, Shomura Y, Bracher A, Hartl FU (2006) Molecular chaperones of the Hsp110 family act as nucleotide exchange factors of Hsp70s. EMBO J 25:2519–2528
113. Arakawa A, Handa N, Ohsawa N, Shida M, Kigawa T, Hayashi F, Shirouzu M, Yokoyama S (2010) The C-terminal BAG domain of BAG5 induces conformational changes of the Hsp70 nucleotide-binding domain for ADP-ATP exchange. Structure 18:309–319
114. Stevens SY, Cai S, Pellecchia M, Zuiderweg ER (2003) The solution structure of the bacterial HSP70 chaperone protein domain DnaK(393-507) in complex with the peptide NRLLLTG. Protein Sci 12:2588–2596
115. Fernandez-Saiz V, Moro F, Arizmendi JM, Acebron SP, Muga A (2006) Ionic contacts at DnaK substrate binding domain involved in the allosteric regulation of lid dynamics. J Biol Chem 281:7479–7488
116. Banecki B, Zylicz M (1996) Real time kinetics of the DnaK/DnaJ/GrpE molecular chaperone machine action. J Biol Chem 271:6137–6143
117. Moro F, Fernandez V, Muga A (2003) Interdomain interaction through helices A and B of DnaK peptide binding domain. FEBS Lett 533:119–123
118. Mayer MP (2010) Gymnastics of molecular chaperones. Mol Cell 39:321–331
119. Zhang Q, Sun X, Watt ED, Al-Hashimi HM (2006) Resolving the motional modes that code for RNA adaptation. Science 311:653–656
120. Cooper A, Dryden DTF (1984) Allostery without conformational change - a plausible model. Eur Biophys J Biophys Lett 11:103–109
121. Lechtenberg BC, Johnson DJD, Freund SMV, Huntington JA (2010) NMR resonance assignments of thrombin reveal the conformational and dynamic effects of ligation. Proc Natl Acad Sci USA 107:14087–14092
122. Itoh K, Sasai M (2010) Entropic mechanism of large fluctuation in allosteric transition. Proc Natl Acad Sci USA 107:7775–7780
123. Tzeng SR, Kalodimos CG (2009) Dynamic activation of an allosteric regulatory protein. Nature 462:368–U139
124. Kern D, Zuiderweg ER (2003) The role of dynamics in allosteric regulation. Curr Opin Struct Biol 13:748–757
125. Stevens SY, Sanker S, Kent C, Zuiderweg ERP (2001) Delineation of the allosteric mechanism of a cytidylyltransferase exhibiting negative cooperativity. Nat Struct Biol 8:947–952
126. Maler L, Blankenship J, Rance M, Chazin WJ (2000) Site-site communication in the EF-hand Ca2+-binding protein calbindin D9k. Nat Struct Biol 7:245–250
127. Han WJ, Christen P (2004) cis-Effect of DnaJ on DnaK in ternary complexes with chimeric DnaK/DnaJ-binding peptides. FEBS Lett 563:146–150
128. Farr CD, Galiano FJ, Witt SN (1995) Large activation energy barriers to chaperone-peptide complex formation and dissociation. Biochemistry 34:15574–15582
129. Farr CD, Witt SN (1997) Kinetic evidence for peptide-induced oligomerization of the molecular chaperone DnaK at heat shock temperatures. Biochemistry 36:10793–10800
130. Farr CD, Slepenkov SV, Witt SN (1998) Visualization of a slow, ATP-induced structural transition in the bacterial molecular chaperone DnaK. J Biol Chem 273:9744–9748
131. Farr CD, Witt SN (1999) ATP lowers the activation enthalpy barriers to DnaK-peptide complex formation and dissociation. Cell Stress Chaperones 4:77–85
132. Varley P, Gronenborn AM, Christensen H, Wingfield PT, Pain RH, Clore GM (1993) Kinetics of folding of the all-beta sheet protein interleukin-1 beta. Science 260:1110–1113
133. Pierpaoli EV, Sandmeier E, Baici A, Schonfeld HJ, Gisler S, Christen P (1997) The power stroke of the DnaK/DnaJ/GrpE molecular chaperone system. J Mol Biol 269:757–768
134. Han WJ, Christen P (2003) Interdomain communication in the molecular chaperone DnaK. Biochem J 369:627–634

135. Siegenthaler RK, Christen P (2006) Tuning of DnaK chaperone action by nonnative protein sensor DnaJ and thermosensor GrpE. J Biol Chem 281:34448–34456
136. Goloubinoff P, Mogk A, Zvi AP, Tomoyasu T, Bukau B (1999) Sequential mechanism of solubilization and refolding of stable protein aggregates by a bichaperone network. Proc Natl Acad Sci USA 96:13732–13737
137. Packschies L, Theyssen H, Buchberger A, Bukau B, Goody RS, Reinstein J (1997) GrpE accelerates nucleotide exchange of the molecular chaperone DnaK with an associative displacement mechanism. Biochemistry 36:3417–3422
138. Xu Z, Page RC, Gomes MM, Kohli E, Nix JC, Herr AB, Patterson C, Misra S (2008) Structural basis of nucleotide exchange and client binding by the Hsp70 cochaperone Bag2. Nat Struct Mol Biol 15:1309–1317
139. Schuermann JP, Jiang JW, Cuellar J, Llorca O, Wang LP, Gimenez LE, Jin SP, Taylor AB, Demeler B, Morano KA, Hart PJ, Valpuesta JM, Lafer EM, Sousa R (2008) Structure of the Hsp110: Hsc70 nucleotide exchange machine. Mol Cell 31:232–243
140. Kabani M, McLellan C, Raynes DA, Guerriero V, Brodsky JL (2002) HspBP1, a homologue of the yeast Fes1 and Sls1 proteins, is an Hsc70 nucleotide exchange factor. FEBS Lett 531:339–342
141. Grimshaw JPA, Jelesarov I, Siegenthaler RK, Christen P (2003) Thermosensor action of GrpE - the DnaK chaperone system at heat shock temperatures. J Biol Chem 278:19048–19053
142. Brehmer D, Gassler C, Rist W, Mayer MP, Bukau B (2004) Influence of GrpE on DnaK-substrate interactions. J Biol Chem 279:27957–27964
143. Rudiger S, Schneider-Mergener J, Bukau B (2001) Its substrate specificity characterizes the DnaJ co-chaperone as a scanning factor for the DnaK chaperone. EMBO J 20:1042–1050
144. Rudiger S, Germeroth L, Schneider-Mergener J, Bukau B (1997) Substrate specificity of the DnaK chaperone determined by screening cellulose-bound peptide libraries. EMBO J 16:1501–1507
145. Feifel B, Schonfeld HJ, Christen P (1998) D-peptide ligands for the co-chaperone DnaJ. J Biol Chem 273:11999–12002
146. Suzuki H, Noguchi S, Arakawa H, Tokida T, Hashimoto M, Satow Y (2010) Peptide-binding sites as revealed by the crystal structures of the human Hsp40 Hdj1 C-terminal domain in complex with the octapeptide from human Hsp70. Biochemistry 49:8577–8584
147. Li JZ, Oian XG, Sha B (2003) The crystal structure of the yeast Hsp40 Ydj1 complexed with its peptide substrate. Structure 11:1475–1483
148. Pellecchia M, Szyperski T, Wall D, Georgopoulos C, Wuthrich K (1996) NMR structure of the J-domain and the Gly/Phe-rich region of the Escherichia coli DnaJ chaperone. J Mol Biol 260:236–250
149. Genevaux P, Fau-Schwager F, Fau K, Georgopoulos C, Kelley W (2002) Scanning mutagenesis identifies amino acid residues essential for the in vivo activity of the Escherichia coli DnaJ (Hsp40) J-domain. Genetics 162:1045–1053
150. Wall D, Zylicz M, Georgopoulos C (1994) The NH2-terminal 108 amino acids of the Escherichia coli DnaJ protein stimulate the ATPase activity of DnaK and are sufficient for lambda replication. J Biol Chem 269:5446–5451
151. Greene MK, Maskos K, Landry SJ (1998) Role of the J-domain in the cooperation of Hsp40 with Hsp70. Proc Natl Acad Sci USA 95:6108–6113
152. Ahmad A, Bhattacharya A, McDonald RA, Cordes M, Ellington B, Bertelsen EB, Zuiderweg ER (2011) Heat shock protein 70 kDa chaperone/DnaJ cochaperone complex employs an unusual dynamic interface. Proc Natl Acad Sci USA 108:18966–18971
153. Wittung-Stafshede P, Guidry J, Horne BE, Landry SJ (2003) The J-domain of Hsp40 couples ATP hydrolysis to substrate capture in Hsp70. Biochemistry 42:4937–4944
154. Huang K, Flanagan JM, Prestegard JH (1999) The influence of C-terminal extension on the structure of the "J-domain" in E. coli DnaJ. Protein Sci 8:203–214

155. Cajo GC, Horne BE, Kelley WL, Schwager F, Georgopoulos C, Genevaux P (2006) The role of the DIF motif of the DnaJ (Hsp40) co-chaperone in the regulation of the DnaK (Hsp70) chaperone cycle. J Biol Chem 281:12436–12444
156. Suh WC, Burkholder WF, Lu CZ, Zhao X, Gottesman ME, Gross CA (1998) Interaction of the Hsp70 molecular chaperone, DnaK, with its cochaperone DnaJ. Proc Natl Acad Sci USA 95:15223–15228
157. Suh WC, Lu CZ, Gross CA (1999) Structural features required for the interaction of the Hsp70 molecular chaperone DnaK with its cochaperone DnaJ. J Biol Chem 274:30534–30539
158. Wall D, Zylicz M, Georgopoulos C (1995) The conserved G/F motif of the DnaJ chaperone is necessary for the activation of the substrate binding properties of the DnaK chaperone. J Biol Chem 270:2139–2144
159. Karzai AW, McMacken R (1996) A bipartite signaling mechanism involved in DnaJ-mediated activation of the Escherichia coli DnaK protein. J Biol Chem 271:11236–11246
160. Pierpaoli EV, Sandmeier E, Schonfeld HJ, Christen P (1998) Control of the DnaK chaperone cycle by substoichiometric concentrations of the co-chaperones DnaJ and GrpE. J Biol Chem 273:6643–6649
161. Horne BE, Li TF, Genevaux P, Georgopoulos C, Landry SJ (2010) The Hsp40 J-domain stimulates Hsp70 when tethered by the client to the ATPase domain. J Biol Chem 285:21679–21688
162. Yochem J, Uchida H, Sunshine M, Saito H, Georgopoulos CP, Feiss M (1978) Genetic-analysis of 2 genes, DnaJ and DnaK, necessary for Escherichia-coli and Bacteriophage-lambda DNA-eeplication. Mol Gen Genet 164:9–14
163. Patury S, Miyata Y, Gestwicki JE (2009) Pharmacological targeting of the Hsp70 chaperone. Curr Top Med Chem 9:1337–1351
164. Nihei T, Sato N, Takahashi S, Ishikawa M, Sagae S, Kudo R, Kikuchi K, Inoue A (1993) Demonstration of selective protein complexes of p53 with 73 kDa heat shock cognate protein, but not with 72 kDa heat shock protein in human tumor cells. Cancer Lett 73:181–189
165. Fourie AM, Hupp TR, Lane DP, Sang BC, Barbosa MS, Sambrook JF, Gething MJ (1997) HSP70 binding sites in the tumor suppressor protein p53. J Biol Chem 272:19471–19479
166. Zylicz M, King FW, Wawrzynow A (2001) Hsp70 interactions with the p53 tumour suppressor protein. EMBO J 20:4634–4638
167. Wadhwa R, Yaguchi T, Hasan MK, Mitsui Y, Reddel RR, Kaul SC (2002) Hsp70 family member, mot-2/mthsp70/GRP75, binds to the cytoplasmic sequestration domain of the p53 protein. Exp Cell Res 274:246–253
168. Bienemann AS, Lee YB, Howarth J, Uney JB (2008) Hsp70 suppresses apoptosis in sympathetic neurones by preventing the activation of c-Jun. J Neurochem 104:271–278
169. Hui-Qing X, Jian-da Z, Xin-Min N, Yan-Zhong Z, Cheng-Qun L, Quan-Yong H, Yi X, Babu Pokharel P, Shao-Hua W, Dan X (2008) HSP70 inhibits burn serum-induced apoptosis of cardiomyocytes via mitochondrial and membrane death receptor pathways. J Burn Care Res 29:512–518
170. Guo F, Sigua C, Bali P, George P, Fiskus W, Scuto A, Annavarapu S, Mouttaki A, Sondarva G, Wei S, Wu J, Djeu J, Bhalla K (2005) Mechanistic role of heat shock protein 70 in Bcr-Abl-mediated resistance to apoptosis in human acute leukemia cells. Blood 105:1246–1255
171. Gyrd-Hansen M, Nylandsted J, Jaattela M (2004) Heat shock protein 70 promotes cancer cell viability by safeguarding lysosomal integrity. Cell Cycle 3:1484–1485
172. Didelot C, Lanneau D, Brunet M, Joly AL, De Thonel A, Chiosis G, Garrido C (2007) Anti-cancer therapeutic approaches based on intracellular and extracellular heat shock proteins. Curr Med Chem 14:2839–2847
173. Wadhwa R, Takano S, Robert M, Yoshida A, Nomura H, Reddel RR, Mitsui Y, Kaul SC (1998) Inactivation of tumor suppressor p53 by mot-2, a hsp70 family member. J Biol Chem 273:29586–29591

174. Lehman TA, Bennett WP, Metcalf RA, Welsh JA, Ecker J, Modali RV, Ullrich S, Romano JW, Appella E, Testa JR et al (1991) p53 mutations, ras mutations, and p53-heat shock 70 protein complexes in human lung carcinoma cell lines. Cancer Res 51:4090–4096
175. King FW, Wawrzynow A, Hohfeld J, Zylicz M (2001) Co-chaperones Bag-1, Hop and Hsp40 regulate Hsc70 and Hsp90 interactions with wild-type or mutant p53. EMBO J 20:6297–6305
176. Lane DP, Midgley C, Hupp T (1993) Tumour suppressor genes and molecular chaperones. Philos Trans R Soc Lond B Biol Sci 339:369–372, discussion 372-3
177. Vargas-Roig LM, Fanelli MA, López LA, Gago FE, Tello O, Aznar JC, Ciocca DR (1997) Heat shock proteins and cell proliferation in human breast cancer biopsy samples. Cancer Detect Prev 21:441–451
178. Nylandsted J, Wick W, Hirt UA, Brand K, Rohde M, Leist M, Weller M, Jaattela M (2002) Eradication of glioblastoma, and breast and colon carcinoma xenografts by Hsp70 depletion. Cancer Res 62:7139–7142
179. Wadhwa R, Takano S, Taira K, Kaul SC (2004) Reduction in mortalin level by its antisense expression causes senescence-like growth arrest in human immortalized cells. J Gene Med 6:439–444
180. Modica-Napolitano JS, Koya K, Weisberg E, Brunelli BT, Li Y, Chen LB (1996) Selective damage to carcinoma mitochondria by the rhodacyanine MKT-077. Cancer Res 56:544–550
181. Rodina A, Vilenchik M, Moulick K, Aguirre J, Kim J, Chiang A, Litz J, Clement CC, Kang Y, She Y, Wu N, Felts S, Wipf P, Massague J, Jiang X, Brodsky JL, Krystal GW, Chiosis G (2007) Selective compounds define Hsp90 as a major inhibitor of apoptosis in small-cell lung cancer. Nat Chem Biol 3:498–507
182. Massey AJ, Wood M (2010) A novel, small molecule inhibitor of Hsc70/Hsp70 potentiates Hsp90 inhibitor induced apoptosis in HCT116 colon carcinoma cells. Cancer Chemother Pharmacol 66:535–545
183. Ermakova SP, Kang BS, Choi BY, Choi HS, Schuster TF, Ma WY, Bode AM, Dong Z (2006) (-)-Epigallocatechin gallate overcomes resistance to etoposide-induced cell death by targeting the molecular chaperone glucose-regulated protein 78. Cancer Res 66:9260–9269
184. Wadhwa R, Sugihara T, Yoshida A, Nomura H, Reddel RR, Simpson R, Maruta H, Kaul SC (2000) Selective toxicity of MKT-077 to cancer cells is mediated by its binding to the hsp70 family protein mot-2 and reactivation of p53 function. Cancer Res 60:6818–6821
185. Wadhwa R, Takano S, Mitsui Y, Kaul SC (1999) NIH 3 T3 cells malignantly transformed by mot-2 show inactivation and cytoplasmic sequestration of the p53 protein. Cell Res 9:261–269
186. Britten CD, Rowinsky EK, Baker SD, Weiss GR, Smith L, Stephenson J, Rothenberg M, Smetzer L, Cramer J, Collins W, Von Hoff DD, Eckhardt SG (2000) A phase I and pharmacokinetic study of the mitochondrial-specific rhodacyanine dye analog MKT 077. Clin Cancer Res 6:42–49
187. Koo EH, Lansbury PT, Kelly JW (1999) Amyloid diseases: abnormal protein aggregation in neurodegeneration. Proc Natl Acad Sci USA 96:9989–9990
188. Caughey B, Lansbury PT (2003) Protofibrils, pores, fibrils, and neurodegeneration: separating the responsible protein aggregates from the innocent bystanders. Annu Rev Neurosci 26:267–298
189. Selkoe DJ (2003) Folding proteins in fatal ways. Nature 426:900–904
190. Avila J, Lucas JJ, Perez M, Hernandez F (2004) Role of tau protein in both physiological and pathological conditions. Physiol Rev 84:361–384
191. Bramblett GT, Goedert M, Jakes R, Merrick SE, Trojanowski JQ, Lee VMY (1993) Abnormal tau-phosphorylation at ser(396) in Alzheimers disease recapitulates development and contributes to reduced microtubule binding. Neuron 10:1089–1099
192. Geschwind DH (2003) Tau phosphorylation, tangles, and neurodegeneration: the chicken or the egg? Neuron 40:457–460
193. Boutajangout A, Quartermain D, Sigurdsson EM (2010) Immunotherapy targeting pathological tau prevents cognitive decline in a new tangle mouse model. J Neurosci 30:16559–16566

194. Dou F, Netzer WJ, Tanemura K, Li F, Hartl FU, Takashima A, Gouras GK, Greengard P, Xu H (2003) Chaperones increase association of tau protein with microtubules. Proc Natl Acad Sci USA 100:721–726
195. Jinwal UK, Miyata Y, Koren J 3rd, Jones JR, Trotter JH, Chang L, O'Leary J, Morgan D, Lee DC, Shults CL, Rousaki A, Weeber EJ, Zuiderweg ER, Gestwicki JE, Dickey CA (2009) Chemical manipulation of hsp70 ATPase activity regulates tau stability. J Neurosci 29:12079–12088
196. Powers MV, Jones K, Barillari C, Westwood I, van Montfort RLM, Workman P (2010) Targeting HSP70: the second potentially druggable heat shock protein and molecular chaperone? Cell Cycle 9:1542–1550
197. Williamson DS, Borgognoni J, Clay A, Daniels Z, Dokurno P, Drysdale MJ, Foloppe N, Francis GL, Graham CJ, Howes R, Macias AT, Murray JB, Parsons R, Shaw T, Surgenor AE, Terry L, Wang YK, Wood M, Massey AJ (2009) Novel adenosine-derived inhibitors of 70 kDa heat shock protein, discovered through structure-based design. J Med Chem 52:1510–1513
198. Kragol G, Lovas S, Varadi G, Condie BA, Hoffmann R, Otvos L (2001) The antibacterial peptide pyrrhocoricin inhibits the ATPase actions of DnaK and prevents chaperone-assisted protein folding. Biochemistry 40:3016–3026
199. Hohfeld J, Minami Y, Hartl F-U (1995) Hip, a novel cochaperone involved in the eukaryotic Hsc70/Hsp40 reaction cycle. Cell 83:589–598
200. Johnson BD, Schumacher RJ, Ross ED, Toft DO (1998) Hop modulates Hsp70/Hsp90 interactions in protein folding. J Biol Chem 273:3679–3686
201. Connell P, Ballinger CA, Jiang J, Wu Y, Thompson LJ, Hohfeld J, Patterson C (2001) The co-chaperone CHIP regulates protein triage decisions mediated by heat-shock proteins. Nat Cell Biol 3:93–96
202. Burri L, Vascotto K, Fredersdorf S, Tiedt R, Hall MN, Lithgow T (2004) Zim17, a novel zinc finger protein essential for protein import into mitochondria. J Biol Chem 279:50243–50249
203. Wisen S, Bertelsen EB, Thompson AD, Patury S, Ung P, Chang L, Evans CG, Walter GM, Wipf P, Carlson HA, Brodsky JL, Zuiderweg ERP, Gestwicki JE (2010) Binding of a small molecule at a protein-protein interface regulates the chaperone activity of Hsp70-Hsp40. ACS Chem Biol 5:611–622
204. Chang L, Miyata Y, Ung PM, Bertelsen EB, McQuade TJ, Carlson HA, Zuiderweg ER, Gestwicki JE (2011) Chemical screens against a reconstituted multiprotein complex: myricetin blocks DnaJ regulation of DnaK through an allosteric mechanism. Chem Biol 18:210–221
205. Rousaki A, Miyata Y, Jinwal UK, Dickey CA, Gestwicki JE, Zuiderweg ER (2011) Allosteric drugs: the interaction of antitumor compound MKT-077 with human Hsp70 chaperones. J Mol Biol 411:614–632
206. Tikoo A, Shakri R, Connolly L, Hirokawa Y, Shishido T, Bowers B, Ye LH, Kohama K, Simpson RJ, Maruta H (2000) Treatment of ras-induced cancers by the F-actin-bundling drug MKT-077. Cancer J 6:162–168
207. Koya K, Li Y, Wang H, Ukai T, Tatsuta N, Kawakami M, Shishido, Chen LB (1996) MKT-077, a novel rhodacyanine dye in clinical trials, exhibits anticarcinoma activity in preclinical studies based on selective mitochondrial accumulation. Cancer Res 56:538–543
208. O'Leary JC, Li QY, Marinec P, Blair LJ, Congdon EE, Johnson AG, Jinwal UK, Koren J, Jones JR, Kraft C, Peters M, Abisambra JF, Duff KE, Weeber EJ, Gestwicki JE, Dickey CA (2010) Phenothiazine-mediated rescue of cognition in tau transgenic mice requires neuroprotection and reduced soluble tau burden. Mol Neurodegener 5:45
209. Dickey CA, Koren J, Zhang YJ, Xu YF, Jinwal UK, Birnbaum MJ, Monks B, Sun M, Cheng AQ, Pattersonl C, Bailey RM, Dunmore J, Soresh S, Leon C, Morgan D, Petrucelli L (2008) Akt and CHIP coregulate tau degradation through coordinated interactions. Proc Natl Acad Sci USA 105:3622–3627

210. Arnone A, Perutz MF (1974) Structure of inositol hexaphosphate-human deoxyhemoglobin complex. Nature 249:34–36
211. Morris G, Goodsell D, Pique M, Lindstrom W, Huey R, Forli S, Hart W, Halliday S, Belew R, Olson A (2010) AutoDock Version 4.2
212. Case DA, Cheatham TE 3rd, Darden T, Gohlke H, Luo R, Merz KM Jr, Onufriev A, Simmerling C, Wang B, Woods RJ (2005) The Amber biomolecular simulation programs. J Comput Chem 26:1668–1688
213. Fogolari F, Brigo A, Molinari H (2003) Protocol for MM/PBSA molecular dynamics simulations of proteins. Biophys J 85:159–166